

3 High-Order Parameterization of Stable/Unstable Manifolds 4 for Long Periodic Orbits of Maps*

5 J. L. Gonzalez[†] and J. D. Mireles James[†]
6

7 **Abstract.** This paper develops seminumerical methods for computing high-order polynomial approximations of
8 stable/unstable manifolds attached to long periodic orbits in discrete time dynamical systems. Our
9 approach extends a standard multiple shooting scheme for periodic orbits, allowing us to compute
10 invariant manifolds for periodic orbits without considering compositions of the map. This leads
11 to a system of conjugacy equations characterizing the complete collection of chart maps, with one
12 chart attaching a local stable/unstable manifold to each point along the periodic orbit. We develop a
13 formal series solution for the system of conjugacy equations and show that the coefficients of the series
14 are determined by recursively solving certain linear systems of equations. We derive the recursive
15 equations for a number of example problems in dimensions two and three, with both polynomial and
16 transcendental nonlinearities, and present some numerical results which illustrate the utility of the
17 method. We also highlight some technical issues such as controlling the decay rate of the coefficients
18 and managing truncation errors via a posteriori indicators.

19 **Key words.** parameterization method, periodic orbits of maps, multiple shooting, stable unstable manifolds

20 **AMS subject classifications.** 37, 37D, 37M

21 **DOI.** 10.1137/16M1090041
22

23
24 **1. Introduction.** In this work we compute high-order polynomial approximations of local
25 stable/unstable manifolds attached to periodic orbits in discrete time dynamical systems. Our
26 approach is based on the parameterization method of [12, 13, 14], which is a general functional
27 analytic framework for studying invariant manifolds. The main idea of the parameterization
28 method is to look for chart maps which satisfy certain invariance equations. In the case of
29 stable/unstable manifolds, this invariance equation conjugates the nonlinear dynamics near
30 the fixed point to a simple polynomial model. (In fact, often we can arrange for the polyno-
31 mial to be linear, see (4) and also Remark 2.6). The parameterization method recovers the
32 dynamics on the invariant manifold in addition to the embedding, and moreover, the chart is
33 not required to be the graph of a function—hence it is possible to follow folds in the embed-
34 ding. The invariance equation also provides a convenient notion of defect, which is exploited
35 for a posteriori error analysis. The main goal of the present work is to develop a parameteri-
36 zation method optimized for periodic problems and to demonstrate that this method leads to
37 efficient numerical implementations.

*Received by the editors August 19, 2016; accepted for publication (in revised form) by J. van den Berg May 15, 2017; published electronically DATE.

<http://www.siam.org/journals/siads/x-x/M109004.html>

Funding: This research was partially supported by NSF grant DMS 1318172.

[†]Department of Mathematical Sciences, Florida Atlantic University, Boca Raton, FL 33431 (jorgegonzale2013@fau.edu, jmirelesjames@fau.edu).

38 A period- N orbit for a map $f: \mathbb{R}^M \rightarrow \mathbb{R}^M$ is a fixed point of the map f^N (f is composed
 39 with itself N times), and in principle one could compute invariant manifolds for period- N
 40 points by applying the parameterization method to the map f^N . In practice, however, the
 41 complexity of the composition f^N grows exponentially in N . The novelty of the present work
 42 is a *composition-free* parameterization method for invariant manifolds attached to periodic
 43 points. The idea is to extend the usual multiple shooting scheme for the periodic orbit itself
 44 to the invariance equation describing the manifold.

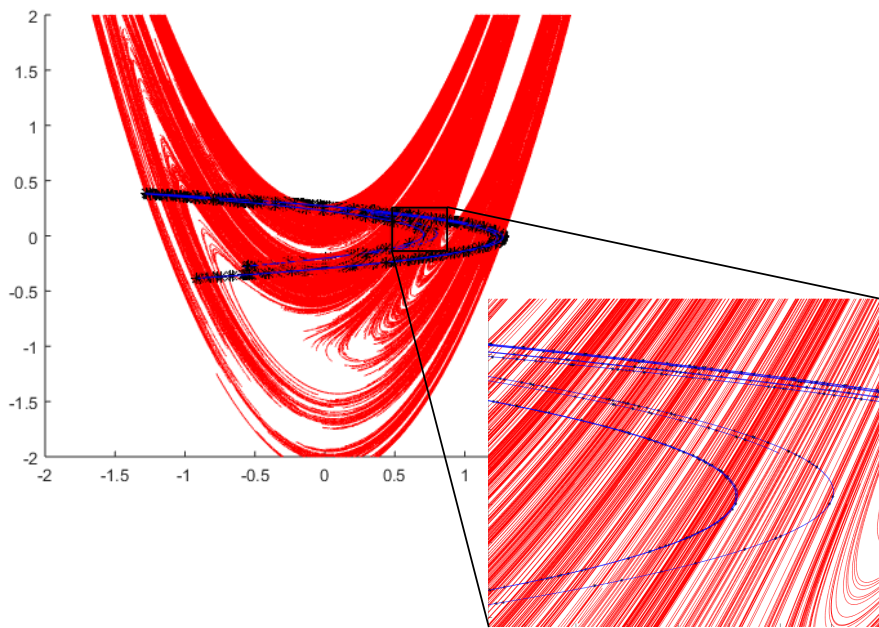
45 More precisely if $p_1, \dots, p_N \in \mathbb{R}^M$ is a periodic orbit with $m \leq M$ stable (or unstable)
 46 eigenvalues, then our method simultaneously finds the Taylor approximations of some func-
 47 tions $P_1, \dots, P_N: \mathbb{R}^m \rightarrow \mathbb{R}^M$ in which P_j parameterizes a local stable (or unstable) manifold
 48 attached to p_j for each $1 \leq j \leq N$. The Taylor approximation is computed numerically
 49 to any desired order. Just as in a multiple shooting scheme for the periodic orbit itself, our
 50 system of invariance equations involves no compositions, and hence the nonlinearity determin-
 51 ing the stable/unstable manifold for the periodic orbit is only as complicated as the original
 52 nonlinearity of the model (see (15)).

53 To illustrate the utility of the method, we implement it for several application problems in
 54 dimensions two and three. We discuss a number of computations for one- and two-dimensional
 55 manifolds associated with periodic orbits of periods up to 100 for a planar and spatial Hénon-
 56 type map. We also show that application of the method is not limited to polynomial maps by
 57 computing stable/unstable manifolds for some periodic orbits of the “standard map,” which
 58 is a system having a trigonometric nonlinearity.

59 *Remark 1.1 (periodic orbits and their stable/unstable manifolds in applied dynamical systems*
 60 *theory).* Periodic orbits are fundamental objects of interest in the qualitative theory of dy-
 61 namical systems. For example, hyperbolic periodic orbits are dense in chaotic sets such as
 62 topological horseshoes and many strange attractors [71, 73]. Studying the set of points in
 63 which the stable/unstable manifolds intersect leads to bounds on topological entropy and a
 64 better understanding of mixing in the system [6, 32]. In these arguments, the more periodic
 65 orbits one includes the better the entropy bounds obtained [18, 19]. We can study the way
 66 that orbits approach an attractor by considering the local stable manifolds of a large enough
 67 collection of periodic points [77]. The attractor itself is well approximated by the unstable
 68 manifolds of such a collection.

69 The implications of Remark 1.1 are illustrated in Figure 1, where we see the stable mani-
 70 folds (in red) and unstable manifolds (in blue) of a collection of points with periods ranging
 71 from 2 to 16 near the Hénon attractor. Points in phase space approach the attractor along
 72 the red curves, while the blue curves describe well the structure of the attractor. (See Remark
 73 1.2 below for more details.)

74 The interested reader could compare the results shown in Figure 1 to similar results
 75 discussed in [66, 78]. In particular, see the bottom right frame of Figure 7 in the former
 76 reference and the bottom right frame of Figure 4 in the latter. These figures illustrate the
 77 results of backward iterating (11 iterates) a local parameterization of the stable manifold of
 78 a fixed point (period one orbit) of the Hénon map. Our Figure 1 provides a much more
 79 dense view of the hyperbolic structure but involves no iteration of the map; i.e., no continu-
 80 ation methods have been applied to the local parameterizations. This highlights the value of

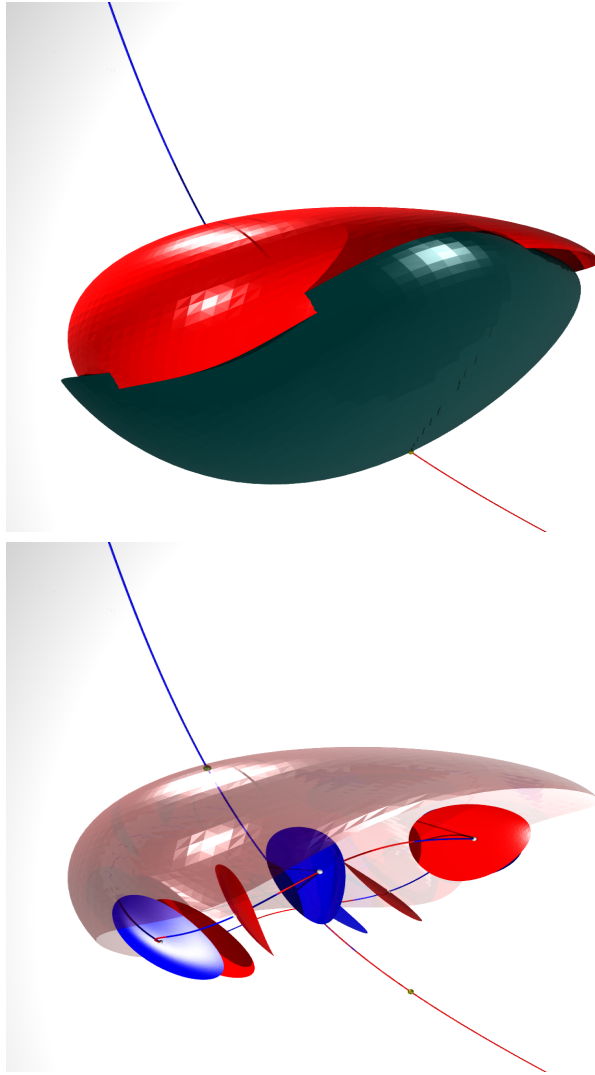


91 **Figure 1.** *Periodic orbits and their attached invariant manifolds for the Hénon map. The figure illustrates*
 92 *the parameterized local unstable/stable manifolds for a collection of orbits having period between 2 and 16. The*
 93 *periodic orbits are black, unstable manifolds are blue, and stable manifolds are red. Orbits approach the Hénon*
 94 *attractor along the (red) stable manifolds. The unstable manifolds (blue) outline the attractor itself. The picture*
 95 *makes it clear that the stable/unstable manifolds intersect many times, giving rise to heteroclinic/homoclinic*
 96 *tangles. The picture is generated by evaluating a collection of polynomial parameterizations for the local sta-*
 97 *ble/unstable manifolds of the periodic orbits, which does not involve any iteration of the map/continuation*
 98 *algorithms. Computations for the Hénon map are discussed in more detail in section 4.3.*

81 the parameterization method developed in the present work but also suggests what could be
 82 achieved in future studies by combining our local methods with globalization techniques such
 83 as those of [66, 78].

84 We must stress again that the idea of using multiple shooting schemes to study periodic
 85 dynamics is standard, having been used to great effect by a number of authors. See, for
 86 example, the study of [75] on computer-assisted analysis of stability regions for the quadratic
 87 map, the studies of [6, 32] on computer-assisted existence proofs for periodic orbits of maps
 88 (the former reference even studies infinite-dimensional discrete time systems), and the more
 89 theoretical study of [28]. The present work extends standard multiple shooting analysis to the
 90 problem of computing local stable/unstable manifolds.

107 *Remark 1.2 (illustration of results).* Figures 1 and 2 illustrate some results obtained using
 108 the methods of the present work. Figure 1 shows parameterized local stable/unstable mani-
 109 folds attached to a collection of periodic orbits for the Hénon map at the classical parameter
 110 values. More precisely, the collection contains 1 period two, 1 period four, 2 period six, 4
 111 period seven, 7 period eight, 6 period nine, 10 period ten, 14 period eleven, 13 period twelve,
 112 23 period thirteen, 9 period fourteen, 21 period fifteen, and 14 period sixteen orbits. Each



99 **Figure 2.** *Vortex bubble and period four subbubble in the Lomelí map: Top: two-dimensional unstable (blue)*
 100 *and two-dimensional stable (red) manifolds attached to the fixed points of the Lomelí map. One-dimensional*
 101 *manifolds are also shown. The two-dimensional manifolds form a “bubble” which encloses all the invariant*
 102 *dynamics of the system. Bottom: dynamics inside the bubble. We locate a pair of period four saddles. The*
 103 *stable/unstable manifolds of the period four orbits form “subbubbles.” We compute polynomial parameterization*
 104 *of the one- and two-dimensional manifolds for the period four points using the techniques of the present work.*
 105 *Again, no continuation scheme has been applied to the local parameterizations illustrated in this figure. These*
 106 *computations are discussed further in section 4.5.*

113 manifold is approximated to Taylor order 25, and the decay rate of the Taylor coefficients
 114 is controlled adaptively to ensure that the last coefficients in this expansion are small. A
 115 posteriori error bounds for each manifold are below 10^{-14} .

116 The second figure shows results from a similar computation involving two fixed points and
 117 two period four orbits of the three-dimensional Lomelí map. This map preserves volume, and

118 hence there are no attractors. Deliberate computations of hyperbolic structures, such as the
 119 ones developed in the present work, facilitate better understanding of the orbit structure of
 120 such systems. The manifolds are approximated to Taylor order 25, and the a posteriori error
 121 is small. More details for these and other computations are found in section 4.

122 The curves and surfaces shown in the figures are obtained by evaluating polynomial ap-
 123 proximations of the local invariant manifolds. The polynomials are computed using the meth-
 124 ods developed in section 3 and implemented as discussed in section 4. The computations
 125 illustrated in the figures, and discussed throughout the present work, make no use of numeri-
 126 cal continuation or globalization methods for the local manifolds. This is not to say that local
 127 parameterizations should never be globalized. Rather, the present work focuses on results
 128 which can be achieved priori to continuation/globalization. We leave to a future study the
 129 task of continuing our results.

130 We make an effort to work out quite explicitly the derivation of the recursion relations
 131 defining the Taylor series coefficients of our polynomial approximations, as it is hoped that
 132 the present work constitutes a stand-alone exposition in this sense. Nevertheless these formal
 133 series arguments can be automated using software packages such as those discussed in [45, 59].
 134 Development of general-purpose software, however, is beyond the scope of the present study.

135 *Remark 1.3 (a posteriori analysis and validated numerics).* As already mentioned above,
 136 one of the strengths of the parameterization method is that it provides a notion of a poste-
 137 riori error (or defect). In other words, since the desired parameterizations solve an operator
 138 equation, we can always plug our approximate solution into the equation, and asses (via some
 139 convenient choice of norm) how close the result is to zero. In the present work we use the a
 140 posteriori error as an indicator of the quality of our computations.

141 Of course small defects do not imply small truncation errors, and it is desirable to have a
 142 more refined a posteriori analysis. Indeed, via a blend of pen- and- paper analysis with delib-
 143 erate control of round-off errors, it is possible to obtain mathematically rigorous computer-
 144 assisted error bounds associated with the polynomial approximations. Several works in this
 145 vein, for both finite- and infinite-dimensional dynamical systems, are [10, 43, 44, 63, 65, 76].
 146 Developing validated numerics for the parameterization method of the present work is the
 147 topic of an upcoming study by the authors [34].

148 **2. Background.** This section reviews some basic notions from the qualitative theory
 149 of dynamical systems and provides a brief review of the parameterization method for sta-
 150 ble/unstable manifolds of fixed points. The reader familiar with the parameterization method
 151 may want to skip ahead to section 3 and refer back to this section only as needed. The reader
 152 wishing to review the parameterization method may want to skim section 2.2.

153 Let $x = (x_1, \dots, x_M) \in \mathbb{R}^M$ denote a point in Euclidean M -space, and endow \mathbb{R}^M with
 154 the norm

$$\|x\| := \max_{1 \leq j \leq M} |x_j|,$$

157 where $|\cdot|$ denotes the usual absolute value. Let

$$B_r^M(x) := \{y \in \mathbb{R}^M : \|x - y\| < r\}$$

160 denote the ball (actually, cube) of radius r about x in this norm. If $E \subset \mathbb{R}^M$ is compact and
 161 $x \in \mathbb{R}^M$, define

$$162 \quad d(x, E) := \inf_{y \in E} \|x - y\|,$$

163
 164 the distance from x to E .

165 When discussing power series, we employ the following notation. If $P: \mathbb{R}^m \rightarrow \mathbb{R}^M$ is
 166 analytic at $p_0 \in \mathbb{R}^M$, then P has a power series representation

$$167 \quad P(\theta) = \sum_{|\alpha|=0}^{\infty} p_{\alpha} \theta^{\alpha} = \sum_{\alpha_1=0}^{\infty} \cdots \sum_{\alpha_m=0}^{\infty} p_{\alpha_1, \dots, \alpha_m} \theta_1^{\alpha_1} \cdots \theta_m^{\alpha_m},$$

168
 169 where $\alpha = (\alpha_1, \dots, \alpha_m) \in \mathbb{N}^m$ is an m -dimensional multi-index,

$$170 \quad |\alpha| := \alpha_1 + \cdots + \alpha_m,$$

171
 172 $p_{\alpha} \in \mathbb{R}^M$ for each α , and

$$173 \quad \theta^{\alpha} := \theta_1^{\alpha_1} \cdots \theta_m^{\alpha_m}.$$

174
 175 **2.1. Stable/unstable manifold for discrete time dynamical systems.** Consider a diffeo-
 176 morphism $f: \mathbb{R}^M \rightarrow \mathbb{R}^M$ with fixed point p . (All of the examples considered in the present
 177 work are in fact analytic maps with analytic inverse.) Suppose that p is a hyperbolic fixed
 178 point of f , i.e., that no eigenvalues of $Df(p)$ lie on the unit circle. Then there are $m_s, m_u \in \mathbb{N}$
 179 with $m_s + m_u = M$, so that $Df(p)$ has m_s stable eigenvalues and m_u unstable eigenvalues
 180 (counted with multiplicity). We then label the eigenvalues as $\lambda_1^s, \dots, \lambda_{m_s}^s, \lambda_1^u, \dots, \lambda_{m_u}^u$ with

$$181 \quad 0 < |\lambda_{m_s}^s| \leq \cdots < |\lambda_1^s| < 1 < |\lambda_1^u| \leq \cdots < |\lambda_{m_u}^u|.$$

182
 183 Let $\xi_1^u, \dots, \xi_{m_u}^u, \xi_1^s, \dots, \xi_{m_s}^s \in \mathbb{R}^M$ denote a choice of linearly independent (possibly general-
 184 ized) eigenvectors.

185 Let $U \subset \mathbb{R}^M$ be an open neighborhood of p . The local stable set of p relative to U is

$$186 \quad W_{\text{loc}}^s(p, U) := \{x \in \mathbb{R}^M : f^n(x) \in U \text{ for all } n \geq 0\}.$$

187
 188 By the stable manifold theorem (see, for example, [67] for discussion and proof) there exists
 189 an open neighborhood $V \subset \mathbb{R}^M$ of p so that

- 190 (i) the local stable set $W_{\text{loc}}^s(p, V)$ is a smooth, embedded, m_s -dimensional disk. If f is
 191 analytic then the embedding is analytic.
- 192 (ii) $W_{\text{loc}}^s(p, V)$ is tangent to the stable eigenspace of $Df(p)$ at p ; i.e., the vectors $\xi_1^s, \dots, \xi_{m_s}^s$
 193 span the tangent space of $W_{\text{loc}}^s(p, V)$ at p .
- 194 (iii) if $x \in W_{\text{loc}}^s(p, V)$, then

$$195 \quad \lim_{n \rightarrow \infty} f^n(x) = p.$$

196

197 We refer to any local stable set $W_{\text{loc}}^s(p, V)$ satisfying (i)–(iii) above as a local stable manifold
 198 for p . We say that $W_{\text{loc}}^s(p)$ is a local stable manifold at p if $W_{\text{loc}}^s(p) = W_{\text{loc}}^s(p, V)$ satisfies (i)–
 199 (iii) above with V some open neighborhood of p . Note that if $W_{\text{loc}}^s(p, V)$ has (i)–(iii) above
 200 and $B_r^M(p) \subset V$, then $W_{\text{loc}}^s(p, B_r^M(p))$ has (i)–(iii) as well; i.e., local stable manifolds are not
 201 unique.

202 Since f is invertible given any local stable manifold $W_{\text{loc}}^s(p, V)$, we can define the set

$$203 \quad (1) \quad W^s(p) = \bigcup_{n=0}^{\infty} f^{-n} [W_{\text{loc}}^s(p)] = \{x \in \mathbb{R}^M \mid f^n(x) \rightarrow p \text{ as } n \rightarrow \infty\}.$$

205 The resulting set $W^s(p)$ is a globally invariant manifold (which may not be an embedded
 206 disk). We refer to $W^s(p)$ as *the* stable manifold of p , as $W^s(p)$ does not depend on the choice
 207 of local stable manifold.

208 With these considerations applied to f^{-1} at p , let us define local unstable manifolds, which
 209 we denote by $W_{\text{loc}}^u(p)$ with analogous definition. (We remark that if p is a hyperbolic fixed
 210 point of a smooth map f , then f^{-1} exists at least locally, and the assumption above that
 211 f is a diffeomorphism on \mathbb{R}^M is not actually needed to define the local unstable manifold.
 212 However, this fact is not used in the present work.) The set

$$213 \quad W^u(p) = \bigcup_{n=0}^{\infty} f^n [W_{\text{loc}}^u(p)] = \{x \in \mathbb{R}^M \mid f^{-n}(x) \rightarrow p \text{ as } n \rightarrow \infty\}$$

215 is a unique globally defined invariant manifold, which we refer to as *the* unstable manifold
 216 of p .

217 **Remark 2.1 (linear approximation of the local stable/unstable manifolds).** Even when the
 218 map $f: \mathbb{R}^M \rightarrow \mathbb{R}^M$ is explicitly known, closed form expressions for the local stable/unstable
 219 manifolds $W_{\text{loc}}^{s,u}(p)$ are rarely available. In applications, we are interested in approximating
 220 these manifolds, and part (ii) of the stable manifold theorem provides a first-order approxi-
 221 mation. More precisely, suppose that the vectors $\xi_1^s, \dots, \xi_{m_s}^s$ are all scaled to have length one,
 222 and define the $M \times m_s$ matrix as

$$223 \quad [\xi_1^s \mid \dots \mid \xi_{m_s}^s] = A_s;$$

225 i.e., A_s is the matrix with columns given by the (generalized) eigenvectors. Then the param-
 226 eterization $P^1: \mathbb{R}^{m_s} \rightarrow \mathbb{R}^M$ given by

$$227 \quad P^1(\theta) := p + A_s \theta, \quad \theta := (\theta_1, \dots, \theta_{m_s})$$

229 approximates $W_{\text{loc}}^s(p)$ to first order. More precisely, let

$$230 \quad B_\delta^{m_s}(0) := \{\theta \in \mathbb{R}^{m_s} : \|\theta\| < \delta\}.$$

232 The restriction of P^1 to $B_\delta^{m_s}(0)$ is a quadratically good approximation of the stable manifold
 233 in the sense that

$$234 \quad \sup_{\theta \in B_\delta^{m_s}(0)} \text{dist}(P^1(\theta), W_{\text{loc}}^s(p)) \leq C \|\theta\|^2,$$

235

though in practice more work is required to obtain estimates on the magnitude of C . Nevertheless, combining the observation above with (1) leads to various algorithms for approximating $W^s(p)$. This point is discussed in more detail in section 2.4. Similar considerations lead to a linear approximation of the local unstable manifold by the unstable (generalized) eigenvectors.

Remark 2.2. To define the linear approximation P^1 in Remark 2.1, it is necessary to fix a choice of scalings for the (generalized) eigenvectors, and of course this choice is not unique. In general the size of the neighborhood on which the linear approximation gives quadratically good approximation depends on the choice of scalings. For example, in Remark 2.1 we would have obtained exactly the same results by taking the (generalized) eigenvectors to have scalings

$$\|\xi_j^s\| = \delta, \quad 1 \leq j \leq m_s,$$

and restricting the domain of P^1 to the unit ball $B_1^{m_s}(0)$.

This nonuniqueness is inherent in many schemes for approximating the stable manifold and plays an important role in what follows. The issue is not surprising, as nonuniqueness appears already in the definition of the local stable manifold (i.e., there is one local stable manifold for every appropriate choice of neighborhood of the fixed point). In the case of the linear approximation, the choice of scalings is more or less arbitrary, and we might as well take unit vectors as in Remark 2.1. However, when we study power series methods, we will see that the freedom to choose the (generalized) eigenvector scalings provides control over the decay rates of the Taylor coefficients. It turns out that manipulating these decay rates is then useful for stabilizing numerical computations.

2.2. Review of the parameterization method. Suppose that f , p , and m_s are as in section 2.1. Throughout the remainder of this section we assume that $m = m_s > 0$ and let $\lambda_1, \dots, \lambda_m$, and ξ_1, \dots, ξ_m denote, respectively, the stable eigenvalues and an associated choice of linearly independent (generalized) eigenvectors. Again, by the stable manifold theorem there is a local stable manifold $W_{\text{loc}}^s(p)$, which is geometrically a smooth embedded disk tangent to the stable (generalized) eigenspace at $p \in \mathbb{R}^M$. We are interested in smooth injective maps $P: B_1^m(0) \rightarrow \mathbb{R}^M$ having

$$(2) \quad P(0) = p \quad \text{and} \quad \frac{\partial}{\partial \theta_j} P(\theta) = \xi_j \quad \text{for each } 1 \leq j \leq m,$$

and

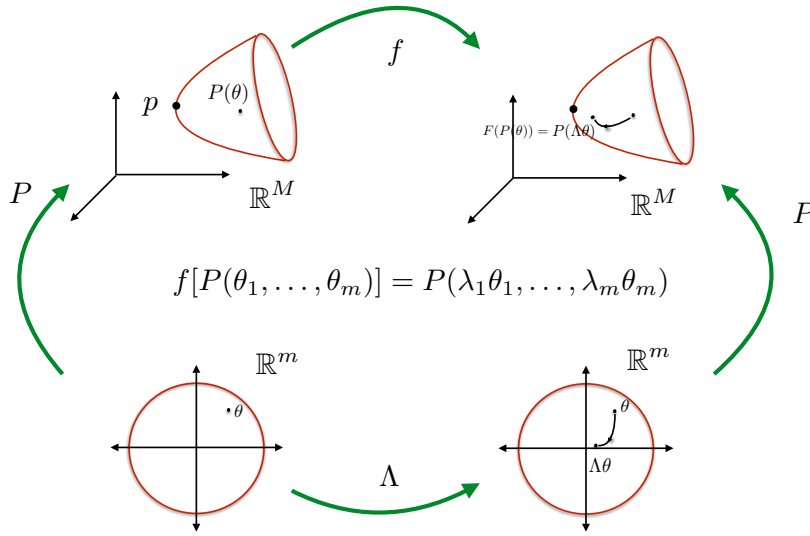
$$(3) \quad P[B_1(0)^m] \subset W^s(p),$$

i.e., charts for the local stable manifold. Clearly if P is one such chart, then any reparameterization of P is again a chart. Thus, the parameterization P just discussed cannot be unique, and we are free to impose additional constraints.

The idea of the *parameterization method* [12, 13, 14] is to look for a smooth function $P: B_1^m(0) \rightarrow \mathbb{R}^M$ satisfying not only the first-order constraints of (2), but also the conjugacy equation

$$(4) \quad f[P(\theta_1, \dots, \theta_m)] = P(\lambda_1 \theta_1, \dots, \lambda_m \theta_m)$$

for all $\theta \in B_1^m(0)$. Several useful results for the parameterization method are summarized below. First we need the following definition.



272 **Figure 3.** Cartoon illustrating the conjugacy relation of (4). Here Λ is the diagonal matrix of eigenvalues,
 273 and f is the nonlinear map. The goal of the parameterization method is to find a chart P which makes the
 274 diagram commute.

282 **Definition 2.3 (nonresonant eigenvalues).** We say that the stable eigenvalues $\lambda_1, \dots, \lambda_m$
 283 are nonresonant if

284
$$\lambda_1^{\alpha_1} \dots \lambda_m^{\alpha_m} \neq \lambda_j \quad \text{with } 1 \leq j \leq m$$

286 for all $\alpha = (\alpha_1, \dots, \alpha_m) \in \mathbb{N}^m$ with $|\alpha| = \alpha_1 + \dots + \alpha_m \geq 2$, that is, if no product of positive
 287 powers of the stable eigenvalues is again a stable eigenvalue.

288 First we note that, despite first appearances, Definition 2.3 imposes only a finite number
 289 of constraints on the eigenvalues. To see this, let

290
$$\mu_* = \min_{1 \leq j \leq m} |\lambda_j| \quad \text{and} \quad \mu^* = \max_{1 \leq j \leq m} |\lambda_j|$$

292 denote, respectively, the smallest and largest moduli of the stable eigenvalues, and note that
 293 for any multi-index $\alpha \in \mathbb{N}^m$, we have the bound

294
$$|\lambda_1^{\alpha_1} \dots \lambda_m^{\alpha_m}| \leq (\mu^*)^{\alpha_1} \dots (\mu^*)^{\alpha_m}$$

 295
$$= (\mu^*)^{|\alpha|}.$$

296 Then a resonance is impossible for any $\alpha \in \mathbb{N}^m$ with

297
$$(\mu_*)^{|\alpha|} > \mu^*,$$

299 and we conclude that a necessary condition for a resonance is that

300 (5)
$$2 \leq |\alpha| \leq \frac{\ln(\mu^*)}{\ln(\mu_*)}.$$

302 Then it is enough to check the resonance conditions only for α as in (5), emphasizing that
 303 ruling out a resonance is a finite check.

304 **Definition 2.4 (eigenvector scalings).** *Suppose that*

$$305 \quad \|\xi_1\| = s_1, \dots, \|\xi_m\| = s_m.$$

306
307 *We refer to the collection of numbers $s_1, \dots, s_m > 0$ as the scalings of the (generalized)*
308 *eigenvectors and write*

$$309 \quad s = \max_{1 \leq j \leq m} (s_j).$$

310
311 The following theorem summarizes a number of basic results. Note that from this point
312 forward we impose the additional assumption that the differential is diagonalizable (see, how-
313 ever, Remark 2.6 below). Proofs of these results can be extracted from the much more general
314 discussion in [12].

315 **Lemma 2.5.** *Let $f: \mathbb{R}^M \rightarrow \mathbb{R}^M$ be an invertible map, and let $p \in \mathbb{R}^M$ be a fixed point of f .*
316 *Suppose that f is differentiable in a neighborhood of p , and assume that the differential $Df(p)$*
317 *is a diagonalizable matrix. Let $\lambda_1, \dots, \lambda_m \in \mathbb{C}$ denote the stable eigenvalues of $Df(p)$, and let*
318 *$\xi_1, \dots, \xi_m \in \mathbb{R}^M$ denote an associated choice of linearly independent eigenvectors.*

- 319 • *If $P: B_1^m(0) \rightarrow \mathbb{R}^M$ is a smooth solution of (4) satisfying the first-order constraints*
320 *given by (2), then P is a chart map for a local stable manifold of p .*
- 321 • *If $\lambda_1, \dots, \lambda_m$ are nonresonant, in the sense of Definition 2.3, then there exists an $\epsilon > 0$*
322 *so that for every choice of eigenvectors with scalings s_1, \dots, s_m as in Definition 2.4*
323 *having $s_1, \dots, s_m \leq \epsilon$, (4) has a solution $P: B_1^m(0) \rightarrow \mathbb{R}^M$ subject to the constraints of*
324 *(2). The solution P is unique up to the choice of the eigenvectors.*
- 325 • *If $f \in C^k(\mathbb{R}^M)$, then $P \in C^k(B_1^m(0), \mathbb{R}^M)$ as well. $k \in \{\infty, \omega\}$ are included in this*
326 *claim.*

327 Now assume that f is analytic near p . Then Lemma 2.5 says that for some choice of eigen-
328 vector scalings a parameterization P solving (4) exists, and that the function P is analytic.
329 Then it is natural to look for a power series solution

$$330 \quad P(\theta) = \sum_{|\alpha|=0}^{\infty} p_\alpha \theta^\alpha.$$

331
332 P satisfies the first-order constraints of (2) if we require that

$$333 \quad p_{\mathbf{0}} = p$$

334
335 and

$$336 \quad p_{e_j} = \xi_j \quad \text{for } 1 \leq j \leq m_s,$$

337
338 where $\mathbf{0} = (0, \dots, 0) \in \mathbb{N}^{m_s}$ is the m_s -dimensional zeroth-order multi-index and $e_j = (0, \dots,$
339 $1, \dots, 0)$ are the standard basis vectors for \mathbb{N}^{m_s} .

340 To work out the higher-order coefficients p_α with $|\alpha| \geq 2$, one expands (4) in terms of this
341 power series, matches like powers of θ , and solves the resulting recurrence equations order by
342 order. This computation results in a *homological equation* of the form

$$343 \quad (6) \quad [Df(p) - \lambda_1^{\alpha_1} \cdots \lambda_{m_s}^{\alpha_{m_s}} \text{Id}] p_\alpha = S_\alpha,$$

where S_α is a function only of the coefficients p_β with $|\beta| < |\alpha|$, and the form of S_α is completely determined by the nonlinearity of f . Observe that (6) provides a linear equation for the Taylor coefficients of the unknown parameterization.

Observe that as long as the eigenvalues are nonresonant in the sense of Definition 2.3, the homological equation (6) is uniquely solvable, and the parameterization P is formally well defined. Once S_α is known explicitly, numerical algorithms for computing the parameterization P are obtained by solving (6) to the desired order.

The derivation of the homological equations are worked out in detail (and in greater generality) in section 3.1 of [12]. Nevertheless for specific examples it is usually desirable (even necessary) to derive the homological equations from scratch in order to obtain the explicit dependence of S_α on the lower-order terms. In section 2.3 we illustrate such a derivation for the composition of the Hénon map with itself. This computation facilitates comparison of the multiple shooting scheme of the present work with a naive application of the parameterization to the composition map as discussed in section 4.2. Other similar computations are found in [30], in sections 2.2 and 2.3 of [62], and in section 3.1 of [15].

Remark 2.6.

- These developments apply to the unstable manifold with only the obvious changes; i.e., one considers exactly the same conjugacy given in (4) and is led to exactly the same homological equation as given by (6), with the only change being that stable eigenvalues/eigenvectors must be replaced by the unstable eigenvalues/eigenvectors. General treatment of the parameterization method is found in the work of [12, 13, 14]. Several papers focusing on numerical aspects of the parameterization method for stable/unstable manifolds of fixed points for maps are [3, 61, 62, 64, 65]. Many additional extensions and applications of these techniques, as well as a thorough discussion of the literature, are found in the recent book of [39].
- Of course in a particular application it is always possible that a resonance will occur. Indeed, for problems with special symmetries, or problems in which we vary a parameter, resonances are sometimes unavoidable. When there is a resonance it is not possible to analytically conjugate to the linear dynamics, even though the map f is analytic. Yet this is not the end of the story, as the method can still succeed after modifying the conjugacy. In fact, one conjugates to a polynomial rather than a linear map, choosing the polynomial to “kill off” the resonant terms. Similar remarks hold in the nondiagonalizable case, i.e., when we have repeated eigenvalues/generalized eigenvectors. These degenerate cases are worked out in full detail in [12]. The end result is that the parameterization method always applies, once resonances are accounted for. See also the work of [76] for numerical implementation, and a posteriori analysis of the resonant cases. More general nonresonance conditions are studied in [20].

2.3. A first worked out example: Homological equations for a fixed point of the Henon-2 map. The Henon map $f: \mathbb{R}^2 \rightarrow \mathbb{R}^2$ is the quadratic polynomial diffeomorphism of the plane given by

$$(7) \quad f(x, y) = \begin{pmatrix} 1 + y - ax^2 \\ bx \end{pmatrix},$$

388 with $a, b \in \mathbb{R}$. The map is invertible with quadratic inverse. For a much more complete
 389 discussion see [41].

390 In this section we consider the mapping $g: \mathbb{R}^2 \rightarrow \mathbb{R}^2$ defined by

$$391 \quad (8) \quad g(x, y) := (f \circ f)(x, y) = \begin{pmatrix} 1 - a + bx - 2ay - ay^2 + 2a^2x^2 + 2a^2yx^2 - a^3x^4 \\ 392 \quad b + by - abx^2 \end{pmatrix},$$

393 i.e., one composition of the Hénon map with itself. Our interest in this map comes from the
 394 fact that if $p_0 \in \mathbb{R}^2$ is fixed for g but not for f , then p_0 is period two for the Hénon map.
 395 Moreover the stable/unstable manifolds of the fixed point p_0 for g are the stable/unstable
 396 manifolds for the period two orbit in the Hénon map.

397 In this section we derive, as an exercise, the homological equations associated with g .
 398 This exercise serves two purposes; first, to review the classical use of the parameterization
 399 as a tool for studying invariant manifolds attached to fixed points; and second, to use the
 400 homological equations derived here in section 4.2 to make some comparisons between a naive
 401 application of the parameterization method to the composition map and the multiple shooting
 402 parameterization method of the present work.

403 Let $Dg(p_0)$ denote the Jacobian differential of g at p_0 , and suppose that $\lambda \in \mathbb{R}$ is a stable
 404 (or unstable) eigenvalue of $Dg(p_0)$. Assume that $Dg(p_0)$ is diagonalizable, and let $\xi \in \mathbb{R}^2$
 405 denote an associated eigenvector. We seek

$$406 \quad P(\theta) = \sum_{n=0}^{\infty} p_n \theta^n = \sum_{n=0}^{\infty} \begin{pmatrix} u_n \\ v_n \end{pmatrix} \theta^n,$$

408 which satisfies the invariance (4). More precisely, we require that

$$409 \quad \begin{pmatrix} u_0 \\ v_0 \end{pmatrix} = p_0 \quad \text{and} \quad \begin{pmatrix} u_1 \\ v_1 \end{pmatrix} = \xi,$$

411 and that P is a solution of

$$412 \quad (9) \quad g(P(\theta)) = P(\lambda\theta).$$

414 Expanding both sides of (9) as power series using Cauchy products and matching like
 415 powers of θ leads to

$$416 \quad \begin{pmatrix} bu_n - 2av_n - a \sum_{k=0}^n v_{n-k}v_k + 2a \sum_{k=0}^n u_{n-k}u_k + 2a^2(v * u * u)_n - a^3(u * u * u * u)_n \\ 417 \quad bv_n - ab \sum_{k=0}^n u_{n-k}u_k \end{pmatrix} \\ 418 \quad = \lambda^n \begin{pmatrix} u_n \\ v_n \end{pmatrix} \\ 419 \quad (10) \\ 420 \\ 421$$

422 for $n \geq 2$, and where (for the sake of brevity) the higher-order Cauchy products are written as

$$423 \quad (v * u * u)_n := \sum_{k=0}^n \sum_{j=0}^k v_{n-k} u_{k-j} u_j$$

424 and

$$426 \quad (u * u * u * u)_n := \sum_{k=0}^n \sum_{j=0}^k \sum_{l=0}^j u_{n-k} u_{k-j} u_{j-l} u_l.$$

427
428 To obtain recurrence relations, we isolate terms of order n , many of which are locked up
429 in the Cauchy products. Thus,

$$430 \quad \sum_{k=0}^n v_{n-k} v_k = 2v_0 v_n + \sum_{k=1}^{n-1} v_{n-k} v_k$$

431 and

$$433 \quad \sum_{k=0}^n u_{n-k} u_k = 2u_0 v_n + \sum_{k=1}^{n-1} u_{n-k} u_k.$$

434 Similarly,

$$436 \quad (v * u * u)_n = 2v_0 u_0 u_n + u_0^2 v_n + \overline{(v * u * u)}_n$$

437 and

$$439 \quad (u * u * u * u)_n = 4u_0^3 u_n + \overline{(u * u * u * u)}_n,$$

440 where

$$442 \quad \overline{(v * u * u)}_n := \sum_{k=0}^n \sum_{j=0}^k \hat{\delta}_{kj}^{nk} v_{n-k} u_{k-j} u_j,$$

$$443 \quad \overline{(u * u * u * u)}_n := \sum_{k=0}^n \sum_{j=0}^k \sum_{l=0}^j \hat{\delta}_{kjl}^{nkj} u_{n-k} u_{k-j} u_{j-l} u_l,$$

$$444 \quad \hat{\delta}_{kj}^{nk} := \begin{cases} 0 & \text{if } k = n \text{ and } j = k, \\ 0 & \text{if } k = n \text{ and } j = 0, \\ 0 & \text{if } k = 0 \text{ and } j = 0, \\ 1 & \text{otherwise} \end{cases}$$

445 and

$$447 \quad \hat{\delta}_{kjl}^{nkj} := \begin{cases} 0 & \text{if } k = n, j = n, \text{ and } l = n, \\ 0 & \text{if } k = n, j = n, \text{ and } l = 0, \\ 0 & \text{if } k = n, j = 0, \text{ and } l = 0, \\ 0 & \text{if } k = 0, j = 0, \text{ and } l = 0, \\ 1 & \text{otherwise.} \end{cases}$$

448
449

450 The point is that these “hatted” products are iterated Cauchy products with terms of order
451 n -removed.

452 We now isolate the terms of order n on the left-hand side and obtain from (10) that

$$(11) \quad \begin{pmatrix} bu_n - 2av_n - 2av_0v_n + 4a^2u_0u_n + 4a^2v_0u_0u_n + 2a^2u_0^2v_n - 4a^3u_0^3u_n \\ bv_n - 2abu_0u_n \end{pmatrix} - \lambda^n \begin{pmatrix} u_n \\ v_n \end{pmatrix} = s_n,$$

455 where the sum

$$(12) \quad s_n := \begin{pmatrix} a \sum_{k=1}^{n-1} v_{n-k}v_k - 2a^2 \sum_{k=1}^{n-1} u_{n-k}u_k - 2a^2 \widehat{(v * u * u)}_n + a^3 \widehat{(u * u * u * u)}_n \\ ab \sum_{k=1}^{n-1} u_{n-k}u_k \end{pmatrix}$$

458 has no dependence on u_n, v_n . Moreover, noting that

$$459 \quad Dg(x, y) = \begin{pmatrix} b + 4a^2x + 4a^2yx - 4a^3x^3 & -2a - 2ay + 2a^2x^2 \\ -2abx & b \end{pmatrix},$$

461 we see that the left-hand side of (11) becomes

$$462 \quad \left[\begin{pmatrix} b + 4a^2u_0 + 4a^2v_0u_0 - 4a^3u_0^3 & -2a - 2av_0 + 2a^2u_0^2 \\ -2abu_0 & b \end{pmatrix} - \lambda^n \begin{pmatrix} 1 & 0 \\ 0 & 1 \end{pmatrix} \right] \begin{pmatrix} u_n \\ v_n \end{pmatrix}$$

$$464 \quad = [Dg(u_0, v_0) - \lambda^n \text{Id}] p_n,$$

466 confirming that the homological have the form claimed in (6) (as they must). More impor-
467 tantly, the calculation provides the explicit form of s_n , which was a priori unknown. Solving
468 the homological equations

$$469 \quad [Dg(u_0, v_0) - \lambda^n \text{Id}] p_n = s_n$$

471 for $2 \leq n \leq K$, with s_n as defined in (12), leads to the K th-order polynomial approximation

$$472 \quad P^K(\theta) = \sum_{n=0}^K p_n \theta^n$$

474 of the local stable/unstable manifold attached to p_0 .

475 **2.4. Related literature: Numerical computation of local stable/unstable manifolds and**
476 **growing or continuing the global manifold.** Two issues have to be considered in any discus-
477 sion of computational methods for stable/unstable manifolds. First is the local computation
478 near the fixed/periodic orbit, and second is the numerical continuation of the local patch.
479 These two steps have their own distinct flavors, and a growing body of literature is devoted
480 to each.

481 The simplest approximation of the local stable/unstable manifold is the linear approxima-
482 tion by the eigenspace already mentioned in Remark 2.2. The linear approximation is widely
483 used and is sufficient for many applications. The idea of studying an invariance equation
484 to obtain the jets of an invariant object appears as early as the work of Poincaré (see, for
485 example, the historical discussion in Appendix A of [14]), and numerical methods based on
486 this idea go back to the work of [30]. See also the lecture notes of [70]. Since then, many
487 authors have expanded this research, and a small (and incomplete) sample of works which
488 focus on high-order numerical approximation of stable/unstable manifolds attached to fixed
489 points of maps includes [3, 9, 43, 62]. These works discuss many additional references. The
490 reader interested in these techniques can consult the recent book of [39] for an overview of
491 the literature, many generalizations to quasi-periodic solutions and their invariant sets, and
492 applications to ODEs.

493 Given a good local approximation of the stable/unstable manifold, one uses continuation
494 techniques such as those discussed in [48, 49] to increase or grow the manifold. For the case of
495 differential equations, we also mention the method of geodesic level sets [37, 50, 51], the method
496 of boundary value problem continuation of trajectories [52], the method of fat trajectories [40],
497 the PDE formulation of [37], as well as the set oriented methods of [21]. The methods of [21]
498 apply to maps as well. In many applications the continuation/globalization methods just
499 mentioned are seeded with the linear approximation of the stable/unstable manifold by the
500 associated stable/unstable eigenspace. Yet none of the methods just mentioned depends on
501 this; that is, they could instead be seeded with larger local patches of manifold given by some
502 high-order approximation, perhaps providing improved results.

503 The two studies [35, 79] explore the possibility of building adaptive continuation methods
504 seeded with high-order parameterizations of the local stable/unstable manifolds. In these
505 works the local manifold is computed to any desired order using the parameterization method
506 (much as in the present work), and then a larger portion of the manifold is grown by adaptively
507 iterating a mesh composed of Bézier triangle patches. These works illustrate nicely what
508 can be achieved by combining the parameterization method with sophisticated continuation
509 techniques.

510 In applications computing stable/unstable manifolds is a first step toward understanding
511 global dynamics of nonlinear systems. We refer, for example, to the numerical studies of
512 global bifurcations and preturbulence for the Lorenz system [1, 27], global consequences of
513 bifurcations at infinity such as α -flips [17], and global invariant manifolds near a Shilnikov
514 bifurcation in a laser model [2]. The interactions between Julia sets and stable/unstable
515 manifolds are studied numerically in [42]. Dynamical transport and design of low energy
516 transport in celestial mechanics, as discussed in [22, 33, 33, 47, 60, 72], is an outstanding
517 example of the use of stable/unstable manifolds in applications. See also the work of [4, 5,
518 23, 24] on weak stability boundaries and geometric instability in Hamiltonian systems, as well
519 the work of [68, 69] on spatial structure of galaxies.

520 Stable/unstable manifolds commonly appear in the geometric theory of dynamical systems
521 as separatrices or transport barriers. We refer, for example, to the work of [55, 56, 57] on
522 generalizations of Melnikov theory based on the study of stable/unstable manifolds and their
523 intersections. Numerical methods for computing connecting orbits are often based on the idea
524 of solving a boundary value problem for orbits beginning on an unstable and terminating on

525 a stable manifold. See, for example, the general numerical methods developed in [8, 26, 31]
 526 and also the lecture notes [25]. We also refer the interested reader to the works of [3, 62, 64]
 527 for discussion of numerical methods which combine high-order parameterization of the local
 528 stable/unstable manifolds with shooting methods for solving discrete time boundary value
 529 problems in order to compute connecting orbits for maps.

530 Of course, the references mentioned in this section barely scratch the surface of the relevant
 531 literature. The discussion above is only meant to provide some motivation and context for
 532 the present work within the existing literature.

533 **3. A parameterization method for periodic orbits.** Let $f: \mathbb{R}^M \rightarrow \mathbb{R}^M$ be a diffeomor-
 534 phism, and recall that f^N denotes the composition of the map f with itself N times (let f^0
 535 be the identity map). A period N point for the map f is a $p \in \mathbb{R}^M$, so that

$$536 \quad f^N(p) = p;$$

537 i.e., p is a fixed point of the map f^N . We say that the point p is a hyperbolic period N point
 538 for f if p is a hyperbolic fixed point of f^N , i.e., if the matrix $Df^N(p)$ has no eigenvalues on
 539 the unit circle. We say that p has least period N if

$$541 \quad f^j(p) \neq f^k(p) \quad \text{for } 1 \leq j \neq k \leq N.$$

542 In both numerical and theoretical considerations of period N points it is often useful to
 543 consider the following “multiple shooting” scheme. We introduce the variables $p = p_1$ and
 544 $f(p_j) = p_{j+1}$ for $j \geq 1$ and look for solutions of the following system of equations:

$$546 \quad f(p_1) = p_2$$

$$547 \quad f(p_2) = p_3$$

$$548 \quad \vdots$$

$$549 \quad f(p_N) = p_1.$$

550 We refer to p_1, \dots, p_N as a periodic orbit for f . Motivated by this system of equations, we
 551 define also the mapping $F: \mathbb{R}^{M \times N} \rightarrow \mathbb{R}^{M \times N}$ by

$$552 \quad (13) \quad F(p_1, \dots, p_N) = \begin{pmatrix} f(p_N) \\ f(p_1) \\ \vdots \\ f(p_{N-1}) \end{pmatrix}$$

553 and note that if $(p_1, \dots, p_N) \in \mathbb{R}^{M \times N}$ is a fixed point of F , then any of the points p_j ,
 554 $1 \leq j \leq N$, is a period N point for f . Moreover if $p_i \neq p_j$ for $i \neq j$, then each of the p_j ,
 555 $1 \leq j \leq N$, has least period N .

556 Note that the differential of F is given by

$$557 \quad DF(p_1, \dots, p_N) = \begin{pmatrix} 0 & 0 & \dots & 0 & Df(p_N) \\ Df(p_1) & 0 & \dots & 0 & 0 \\ 0 & Df(p_2) & \dots & 0 & 0 \\ \vdots & \vdots & \ddots & \vdots & \vdots \\ 0 & 0 & \dots & Df(p_{N-1}) & 0 \end{pmatrix}.$$

559

560 Moreover suppose that $\mathbf{p} = (p_1, \dots, p_N) \in \mathbb{R}^{M \times N}$ is a fixed point of F , and let $\lambda \in \mathbb{C}$ and
 561 $\xi = (\xi_1, \dots, \xi_N) \in \mathbb{R}^{M \times N}$. Then we have the following proposition.

562 **Proposition 3.1.** *Suppose that $\mathbf{p} \in \mathbb{R}^{M \times N}$ is a fixed point of F . Then λ, ξ is an eigenvalue/
 563 eigenvector pair for $DF(\mathbf{p})$ if and only if for each $1 \leq j \leq N$, $\sqrt[N]{\lambda}, \xi_j$ is an eigenvalue/
 564 eigenvector pair for $Df^N(p_j)$.*

565 *Proof.* Note that $\lambda \neq 0$, as f is a diffeomorphism. Moreover each of the matrices $Df(p_j)$
 566 is invertible. Starting with $DF(\mathbf{p})\xi = \lambda\xi$ and rewriting it as the system

$$\begin{aligned} 567 \quad & Df(p_N)\xi_N = \lambda\xi_1 \\ 568 \quad & Df(p_1)\xi_1 = \lambda\xi_2 \\ & \vdots \\ 569 \quad & \\ 570 \quad & Df(p_{N-1})\xi_{N-1} = \lambda\xi_{N-1}, \end{aligned}$$

571 we get that

$$\begin{aligned} 572 \quad & Df(p_{j+1})Df(p_j)\xi_j = \lambda^2\xi_{j+2} \\ & \vdots \\ 573 \quad & \\ 574 \quad & Df(p_{j-1}) \cdots Df(p_1)Df(p_N) \cdots Df(p_j)\xi_j = \lambda^N\xi_j, \end{aligned}$$

575 i.e., $Df^N(p_j)\xi_j = \lambda^N\xi_j$, by the chain rule. Reversing the computation gives the reverse
 576 implication. ■

577 The proposition says that we recover the stability of each of the period N points p_j ,
 578 $1 \leq j \leq N$, by computing the stability of the fixed point \mathbf{p} . Note that the proof also recovers
 579 the classic fact that if p_1, \dots, p_N is a periodic orbit of least period N , then each of the periodic
 580 points has the same eigenvalues. Moreover the periodic orbit is hyperbolic if and only if \mathbf{p} is
 581 a hyperbolic fixed point.

582 **3.1. Composition-free invariance equations.** Continuing the notation established in sec-
 583 tion 3, let $p_1, \dots, p_N \in \mathbb{R}^M$ be a hyperbolic periodic orbit of the smooth map $f: \mathbb{R}^M \rightarrow \mathbb{R}^M$,
 584 and let $\tilde{\lambda}_1, \dots, \tilde{\lambda}_m$ denote the stable eigenvalues of any of the matrices $Df^N(p_j)$, $1 \leq j \leq N$ (as
 585 each of these matrices has the same eigenvalues). Assume that each of the matrices $Df^N(p_j)$,
 586 $1 \leq j \leq N$, is diagonalizable, and let $\tilde{\xi}_1^{(j)}, \dots, \tilde{\xi}_m^{(j)}$ denote a linearly independent choice of
 587 eigenvectors. Motivated by the above considerations for periodic points, we develop a “mul-
 588 tiple shooting” approach to the parameterization of stable/unstable manifolds for a period N
 589 point. Let

$$590 \quad \lambda_j := \left(\tilde{\lambda}_j \right)^{\frac{1}{N}}$$

591 for each $1 \leq j \leq m$.

592 We look for smooth functions $P^{(j)}: B_1^m(0) \rightarrow \mathbb{R}^M$, $1 \leq j \leq N$, satisfying the first-order
 593 constraints

$$594 \quad (14) \quad P^{(j)}(0) = p_j \quad \text{and} \quad \frac{\partial}{\partial \theta_k} P^{(j)}(0) = \xi_k^{(j)}$$

597 for $1 \leq j \leq N$ and $1 \leq k \leq m$, and solve the system of invariance equations

$$\begin{aligned}
 & f(P^{(1)}(\theta_1, \dots, \theta_m)) = P^{(2)}(\lambda_1 \theta_1, \dots, \lambda_m \theta_m) \\
 & f(P^{(2)}(\theta_1, \dots, \theta_m)) = P^{(3)}(\lambda_1 \theta_1, \dots, \lambda_m \theta_m) \\
 & \vdots \\
 & f(P^{(N-1)}(\theta_1, \dots, \theta_m)) = P^{(N)}(\lambda_1 \theta_1, \dots, \lambda_m \theta_m) \\
 & f(P^{(N)}(\theta_1, \dots, \theta_m)) = P^{(1)}(\lambda_1 \theta_1, \dots, \lambda_m \theta_m)
 \end{aligned}
 \tag{15}$$

600 for $\theta_1, \dots, \theta_m \in B_1^m(0)$.

601 The following discussion explains our interest in this system. Suppose that $(P^{(1)}, \dots,$
602 $P^{(N)}(\theta))$ is a solution of the system of (15). Then

$$f[P^{(1)}(\theta_1, \dots, \theta_m)] = P^{(2)}(\lambda_1 \theta_1, \dots, \lambda_m \theta_m),$$

605 so that

$$f\left(f[P^{(1)}(\theta_1, \dots, \theta_m)]\right) = f[P^{(2)}(\lambda_1 \theta_1, \dots, \lambda_m \theta_m)] = P^{(3)}(\lambda_1^2 \theta_1, \dots, \lambda_m^2 \theta_m)$$

608 or

$$f^2[P^{(1)}(\theta_1, \dots, \theta_m)] = P^{(3)}(\lambda_1^2 \theta_1, \dots, \lambda_m^2 \theta_m).$$

611 Proceeding in this way leads to

$$f^k[P^{(1)}(\theta_1, \dots, \theta_m)] = P^{(k+1)}(\lambda_1^k \theta_1, \dots, \lambda_m^k \theta_m)$$

614 for $1 \leq k \leq N-1$, and finally

$$f^N[P^{(1)}(\theta_1, \dots, \theta_m)] = P^{(1)}(\lambda_1^N \theta_1, \dots, \lambda_m^N \theta_m),$$

617 which is

$$f^N[P^{(1)}(\theta_1, \dots, \theta_m)] = P^{(1)}(\tilde{\lambda}_1 \theta_1, \dots, \tilde{\lambda}_m \theta_m),$$

620 so that $P^{(1)}$ satisfies the parameterization conjugacy equation for the composition map f^N .

621 Repeating this computation for each $P^{(k)}$ with $2 \leq k \leq N$ gives the following.

622 *Claim 3.2.* If $P(\theta) := (P^1(\theta_1, \dots, \theta_m), \dots, P^{(N)}(\theta_1, \dots, \theta_m))$ solves the system of equa-
623 tions given by (15), then $P^{(k)}$ parameterizes the local stable manifold at p_k for each $1 \leq k \leq N$.

624 To solve the system of invariance equations, we consider the case when f is analytic and
625 look for formal series solutions

$$P^{(k)}(\theta_1, \dots, \theta_m) = \sum_{|\alpha|=0}^{\infty} p_{\alpha}^{(k)} \theta^{\alpha}$$

628 or

$$P(\theta) = \sum_{|\alpha|=0}^{\infty} p_{\alpha} \theta^{\alpha}, \quad \text{where } p_{\alpha} = \begin{pmatrix} p_{\alpha}^{(1)} \\ \vdots \\ p_{\alpha}^{(N)} \end{pmatrix}.$$

630

631

632 We will see that if $F: \mathbb{R}^{MN} \rightarrow \mathbb{R}^{MN}$ is the map defined in (13), and if $p = (p_1, \dots, p^N) \in \mathbb{R}^{MN}$
 633 denotes the periodic orbit, then the coefficients of P solve homological equations of the form

$$634 \quad (16) \quad [DF(p) - \lambda_1^{\alpha_1} \cdots \lambda_m^{\alpha_m} \text{Id}_{\mathbb{R}^{MN}}] p_\alpha = S_\alpha.$$

636 Here S_α is a nonlinear function of the coefficients $\{p_\beta\}$ with $|\beta| < |\alpha|$, and the form of the
 637 nonlinearity of S_α depends only on the nonlinearity of f (rather than the nonlinearity f^N).
 638 Deriving the explicit form of S_α is a problem-dependent question best illustrated in specific
 639 examples.

640 Note that

$$641 \quad \lambda_1^{\alpha_1} \cdots \lambda_m^{\alpha_m} = \lambda_k$$

643 for some $1 \leq k \leq N$ and some fixed multi-index $(\alpha_1, \dots, \alpha_m) \in \mathbb{Z}^m$ if and only if

$$644 \quad \tilde{\lambda}_1^{\alpha_1} \cdots \tilde{\lambda}_m^{\alpha_m} = \tilde{\lambda}_k,$$

646 with the same data; i.e., the homological equations (16) have a unique solution p_α for each
 647 $\alpha \in \mathbb{N}^m$, $|\alpha| \geq 2$, if and only if the eigenvalues of $Df^N(p_k)$ are nonresonant. Then the
 648 “multiple-shooting” version of the parameterization method is applicable if and only if the
 649 standard version applies to the fixed point of the composition map.

650 **Claim 3.3 (real analytic parameterizations).** By appropriately choosing the eigenvectors, we
 651 can always arrange for the image of the parameterizations to be real.

652 Starting with a real eigenvalue and eigenvector of $Df^N(p_j)$, call it $u_1^{(j)}$, it is easy to see
 653 from the recursive equation $(Df^N(p_j) - \lambda^{Nn} I)u_\alpha^{(j)} = s_\alpha^{(j)}$ that $u_\alpha^{(j)}$ is real for all α . Now we
 654 rewrite $(DF(p_*) - \lambda^n I)u_\alpha = S_\alpha$ as a system using block multiplication, i.e.,

$$655 \quad Df(p_N)u_\alpha^{(N)} - \lambda^\alpha u_\alpha^{(1)} = S_\alpha^{(1)}$$

657 and

$$658 \quad Df(p_j)u_\alpha^{(j)} - \lambda^\alpha u_\alpha^{(j+1)} = S_\alpha^{(j+1)}$$

660 for $j = 1, \dots, N-1$. This system leads to

$$661 \quad (Df(p_{j-1}) \cdots Df(p_1) Df(p_N) \cdots Df(p_j) - \lambda^{N\alpha} I)u_\alpha^{(j)} = \Sigma_\alpha^{(j)},$$

663 that is

$$664 \quad (Df^N(p_j) - \lambda^{N\alpha} I)u_\alpha^{(j)} = \Sigma_\alpha^{(j)},$$

666 where

$$667 \quad \Sigma_\alpha^{(j)} = (Df(p_j) \cdots Df(p_1) Df(p_N) \cdots Df(p_{j+1})) S_\alpha^{(j)} \\ 668 \quad + \lambda^\alpha (Df(p_j) \cdots Df(p_1) Df(p_N) \cdots Df(p_{j+2})) S_\alpha^{(j+1)} \\ 669 \quad + \cdots \\ 670 \quad + \lambda^{(N-1)\alpha} S_\alpha^{(j-1)}.$$

671 Summarizing, we have that

$$672 \quad \Sigma_\alpha^{(j)} = Df^N(p_{j+1})S_\alpha^{(j)} + \lambda^\alpha Df^{N-1}(p_{j+2})S_\alpha^{(j+1)} + \dots + \lambda^{(N-1)\alpha} S_\alpha^{(j-1)}[*].$$

674 Now $(Df^N(p_j) - \lambda^{N\alpha}I)$ is a real matrix, and hence it is enough to ensure that $\Sigma_\alpha^{(j)}$ is real.

675 For $\Sigma_\alpha^{(j)}$, a finite sum of convolution terms the above suggests to multiply $u_1^{(j-1)}$ by λ
 676 \dots and $u_1^{(j+1)}$ by λ^{N-1} . In practice, we multiply $u_1^{(j-1)}$ by a primitive N root of unity ρ
 677 \dots and multiply $u_1^{(j+1)}$ by ρ^{N-1} . Using automatic differentiation, the argument extends to
 678 non-polynomial nonlinearities as well.

679 For simplicity of the argument pick $u_1^{(N)}$ real; then using induction on $[*]$ we show that
 680 $u_\alpha^{(j)}\lambda^{N-j}$ is real for all α and j , and it also shows that multiplying $u_1^{(j)}$ by λ and recomputing
 681 $u_\alpha^{(j)}$ to evaluate $\hat{P}^{(j)}(\theta)$ is equivalent to computing $P^{(j)}(\lambda\theta)$.

682 **Claim 3.4 (nonuniqueness and scaling the eigenvectors).** By appropriately choosing the scal-
 683 ings of the eigenvectors, we can arrange that for Taylor series coefficients of the parameteri-
 684 zations to have whatever exponential decay rate we like.

685 To see this, note that Lemma 2.5 tells us that solutions of (4) are unique up to the choice
 686 of the scalings of the eigenvectors at the fixed point. The same follows for the system given
 687 by (15), precisely because solutions of the system of equations (15) are equivalent to solutions
 688 of (4) for the composition map.

689 Moreover we can work out exactly the effect of rescaling the eigenvectors on the Taylor
 690 coefficients of the solution. To this end, consider

$$691 \quad P^{(k)}(\theta_1, \dots, \theta_m) = \sum_{|\alpha|=0}^{\infty} p_\alpha^{(k)} \theta^\alpha$$

693 for $1 \leq k \leq m$ solving the system of equations (15), and suppose that the eigenvectors
 694 $\xi_j = (p_{e_j}^{(1)}, \dots, p_{e_j}^{(N)})$ have $\|\xi_j\| = 1$. Now choose scalings $0 < \sigma_j$ for $1 \leq j \leq m$, and define the
 695 vector $\sigma = (\sigma_1, \dots, \sigma_m)$, as well as the new collection of functions

$$696 \quad \hat{P}^{(k)}(\theta_1, \dots, \theta_m) = \sum_{|\alpha|=0}^{\infty} \hat{p}_\alpha^{(k)} \theta^\alpha,$$

698 where

$$699 \quad (17) \quad \hat{p}_\alpha^{(k)} = \sigma^\alpha p_\alpha^{(k)}, \quad 1 \leq k \leq m.$$

701 Note that

$$702 \quad \hat{p}_0^{(k)} = \sigma^0 p_0^{(k)} = p_k$$

704 and

$$705 \quad \hat{p}_{e_j}^{(k)} = \sigma^{e_j} p_{e_j}^{(k)} = \sigma_j p_{e_j}^{(k)};$$

707 i.e., \hat{P} satisfies the first-order constraints given by (14).

708 Now define the new variables

$$709 \quad \hat{\theta}_j = \frac{\theta_j}{\sigma_j}$$

710

711 for $1 \leq j \leq m$. Then

$$712 \quad \hat{P}^{(k)}(\hat{\theta}_1, \dots, \hat{\theta}_m) = \sum_{|\alpha|=0}^{\infty} \hat{p}_{\alpha}^{(k)} \hat{\theta}^{\alpha}$$

$$713 \quad = \sum_{|\alpha|=0}^{\infty} \sigma^{\alpha} p_{\alpha}^{(k)} \hat{\theta}^{\alpha}$$

$$714 \quad = \sum_{|\alpha|=0}^{\infty} p_{\alpha}^{(k)} \theta^{\alpha}$$

$$715 \quad = P^{(k)}(\theta_1, \dots, \theta_m).$$

716 Then

$$717 \quad P^{(k)}(\lambda_1 \theta_1, \dots, \lambda_m \theta_m) = f[P^{(k+1)}(\theta_1, \dots, \theta_m)]$$

$$718 \quad = f[\hat{P}^{(k+1)}(\hat{\theta}_1, \dots, \hat{\theta}_m)].$$

719 Combining these observations gives that

$$720 \quad f[\hat{P}^{(k+1)}(\hat{\theta}_1, \dots, \hat{\theta}_m)] = \hat{P}^{(k)}(\lambda_1 \hat{\theta}_1, \dots, \lambda_m \hat{\theta}_m),$$

721

722 i.e., that \hat{P} is the solution of the system given by (15), subject to the linear constraints with
 723 eigenvectors scaled by σ . By uniqueness, \hat{P} is the only such solution. This shows that given
 724 one solution of (15) whose Taylor coefficients are $\{p_{\alpha}\}$, rescaling the eigenvectors by σ leads
 725 to a new solution of (15) whose Taylor coefficients are determined from $\{p_{\alpha}\}$ by (17).

726 **3.2. Formal solution of the invariance equations.** We now study the system of invariance
 727 equations (15) for a number of particular example problems. Our goal is to illustrate the
 728 derivation of the homological equations which are essential for numerically implementing the
 729 parameterization method.

730 **3.2.1. A second worked out example: Stable/unstable manifolds of a period two orbit**
 731 **the for Hénon map using multiple shooting parameterization.** In this section $f: \mathbb{R}^2 \rightarrow \mathbb{R}^2$
 732 denotes the Hénon map defined in (7). Suppose that $p_0, q_0 \in \mathbb{R}^2$ is a saddle-type period two
 733 orbit for f , i.e., that

$$734 \quad f(p_0) = q_0 \quad \text{and} \quad f(q_0) = p_0,$$

735

736 with $p_0 \neq q_0$, that $\tilde{\lambda} \in \mathbb{R}$ has $|\tilde{\lambda}| < 1$, that $\xi, \eta \in \mathbb{R}^2$ have

$$737 \quad Df^2(p_0)\xi = \tilde{\lambda}\xi \quad \text{and} \quad Df^2(q_0)\eta = \tilde{\lambda}\eta,$$

738

739 and that the remaining eigenvalue of $Df^2(p_0)$, $Df^2(q_0)$ is unstable. Define

$$740 \quad \lambda = \sqrt{\tilde{\lambda}}.$$

742 In this setting the system of invariance equations given by (15) reduces to

$$743 \quad (18) \quad \begin{aligned} f(Q(\theta)) &= P(\lambda\theta), \\ f(P(\theta)) &= Q(\lambda\theta). \end{aligned}$$

745 We look for P, Q of the form

$$746 \quad P(\theta) = \sum_{n=0}^{\infty} p_n \theta^n$$

748 and

$$749 \quad Q(\theta) = \sum_{n=0}^{\infty} q_n \theta^n$$

751 and require that

$$752 \quad P(0) = p_0 \quad \text{and} \quad Q(0) = q_0$$

754 (so that q_0, p_0 denote the zeroth Taylor coefficient as well as the periodic orbit) and also that

$$755 \quad P'(0) = p_1 = \xi \quad \text{and} \quad Q'(0) = q_1 = \eta,$$

757 so that P and Q are tangent to the correct eigenspaces.

758 We will derive the explicit form of the homological equation (16). To this end, note that

$$759 \quad P(\lambda\theta) = \sum_{n=0}^{\infty} \lambda^n p_n \theta^n \quad \text{and} \quad Q(\lambda\theta) = \sum_{n=0}^{\infty} \lambda^n q_n \theta^n.$$

761 Writing

$$762 \quad p_n = \begin{pmatrix} p_n^1 \\ p_n^2 \end{pmatrix} \quad \text{and} \quad q_n = \begin{pmatrix} q_n^1 \\ q_n^2 \end{pmatrix}$$

764 for the components of the Taylor coefficients, and employing the Cauchy product for power series, we have

$$766 \quad f(P(\theta)) = \begin{pmatrix} 1 + \sum_{n=0}^{\infty} p_n^2 - \sum_{n=0}^{\infty} \sum_{k=0}^n a p_{n-k}^1 p_k^1 \\ \sum_{n=0}^{\infty} b p_n^1 \end{pmatrix}$$

768 and

$$769 \quad f(Q(\theta)) = \begin{pmatrix} 1 + \sum_{n=0}^{\infty} q_n^2 - \sum_{n=0}^{\infty} \sum_{k=0}^n a q_{n-k}^1 q_k^1 \\ \sum_{n=0}^{\infty} b q_n^1 \end{pmatrix}.$$

770
771

772 Plugging these power series expansions into (18) and matching like powers of θ for $n \geq 2$
 773 leads to

$$774 \quad \begin{pmatrix} q_n^2 - \sum_{k=0}^n a q_{n-k}^1 q_k^1 \\ b q_n^1 \\ p_n^2 - \sum_{k=0}^n a p_{n-k}^1 p_k^1 \\ b p_n^1 \end{pmatrix} = \begin{pmatrix} \lambda^n p_n^1 \\ \lambda^n p_n^2 \\ \lambda^n q_n^1 \\ \lambda^n q_n^2 \end{pmatrix}$$

775
 776 or

$$777 \quad \begin{pmatrix} q_n^2 - 2a q_0^1 q_n^1 - \sum_{k=1}^{n-1} a q_{n-k}^1 q_k^1 \\ b q_n^1 \\ p_n^2 - 2a p_0^1 p_n^1 - \sum_{k=1}^{n-1} a p_{n-k}^1 p_k^1 \\ b p_n^1 \end{pmatrix} = \lambda^n \begin{pmatrix} p_n^1 \\ p_n^2 \\ q_n^1 \\ q_n^2 \end{pmatrix}.$$

778
 779 We move terms of order n to the left, move terms of order less than n to the right, and observe
 780 that the dependence on p_n, q_n is linear. This results in the equations

$$781 \quad (19) \quad \left[\begin{pmatrix} 0 & 0 & -2a q_0^1 & 1 \\ 0 & 0 & b & 0 \\ -2p_0^1 & 1 & 0 & 0 \\ b & 0 & 0 & 0 \end{pmatrix} - \lambda^n \begin{pmatrix} 1 & 0 & 0 & 0 \\ 0 & 1 & 0 & 0 \\ 0 & 0 & 1 & 0 \\ 0 & 0 & 0 & 1 \end{pmatrix} \right] \begin{bmatrix} p_n^1 \\ p_n^2 \\ q_n^1 \\ q_n^2 \end{bmatrix} = \begin{bmatrix} a \sum_{k=1}^{n-1} q_{n-k}^1 q_k^1 \\ 0 \\ a \sum_{k=1}^{n-1} p_{n-k}^1 p_k^1 \\ 0 \end{bmatrix}.$$

782
 783 Letting $F: \mathbb{R}^4 \rightarrow \mathbb{R}^4$ be the map

$$784 \quad F(p_1, p_2, q_1, q_2) = \begin{pmatrix} 1 + q_2 - a q_1^2 \\ b q_1 \\ 1 + p_2 - a p_1^2 \\ b p_1 \end{pmatrix},$$

785
 786 we see that, indeed, (19) has exactly the form promised in (16). The point of working through
 787 the computation above is that we now know explicitly the form of the right-hand side of the
 788 homological equation, and this knowledge is used to implement numerical algorithms.

789 Note that for all $n \geq 2$, λ^n is not an eigenvalue of $DF(p_0, q_0)$. This is because we assumed
 790 that p_0, q_0 is a hyperbolic saddle, and hence the only other eigenvalue has absolute value
 791 greater than one. Then $|\lambda^n| < |\lambda| < 1$ for all $n \geq 2$, and hence λ^n is never an eigenvalue.
 792 Equation (19) is characteristic for $DF(p_0, q_0)$, and we have that solutions exist and are unique

793 for any right-hand side and for as long $n \geq 2$. This is a specific instance of a more general
 794 result, namely that a saddle with exactly one stable eigenvalue is never resonant. Solving (19)
 795 recursively for each $2 \leq n \leq K$ leads to the polynomial approximations

$$796 \quad P^K(\theta) = \sum_{n=0}^K p_n \theta^n \quad \text{and} \quad Q^K(\theta) = \sum_{n=0}^K q_n \theta^n.$$

798 Also note that if we consider instead the unstable eigenvalues, all of the comments above
 799 go through. We discuss numerical methods further in section 4.

800 **3.2.2. The homological equations for a period N point of Hénon.** Suppose now that
 801 $p^1, \dots, p^N \in \mathbb{R}^2$ is a periodic orbit of the Hénon map with least period N , and that $\tilde{\lambda} \in \mathbb{R}$
 802 and $\xi^1, \dots, \xi^N \in \mathbb{R}^2$ have that

$$803 \quad Df^N(p^k)\xi^k = \tilde{\lambda}\xi^k$$

805 for $1 \leq k \leq N$. Define the map

$$806 \quad F(x_1, y_1, x_2, y_2, \dots, x_N, y_N) = \begin{pmatrix} 1 + y_N - ax_N^2 \\ bx_N \\ 1 + y_2 - ax_2^2 \\ bx_2 \\ \vdots \\ 1 + y_1 - ax_1^2 \\ bx_1 \end{pmatrix}.$$

808 Define

$$809 \quad \lambda = \sqrt[N]{\tilde{\lambda}}.$$

811 Note that p^1, \dots, p^N is a fixed point of F and that $\tilde{\lambda}, \xi^1, \dots, \xi^N$ can be computed by finding
 812 eigenvalues/eigenvectors for $DF(p^1, \dots, p^N)$.

813 Let $p_0, p_1 \in \mathbb{R}^{2N}$ be

$$814 \quad p_0 = \begin{pmatrix} p^1 \\ \vdots \\ p^N \end{pmatrix} \quad \text{and} \quad p_1 = \begin{pmatrix} \xi^1 \\ \vdots \\ \xi^N \end{pmatrix}.$$

816 We seek

$$817 \quad P(\theta) = \begin{pmatrix} P^{(1)}(\theta) \\ \vdots \\ P^{(N)}(\theta) \end{pmatrix},$$

819 solving the invariance equation, with

$$820 \quad P^{(k)}(\theta) = \sum_{n=0}^{\infty} p_n^k \theta^n$$

821

822 for $p_n^k \in \mathbb{R}^2$ for $1 \leq k \leq N$. We write $p_n^k = (p_{n,1}^k, p_{n,2}^k)$ to denote the components. Define
 823 $p_n \in \mathbb{R}^{2N}$ by

$$824 \quad p_n = \begin{pmatrix} p_n^1 \\ \vdots \\ p_n^N \end{pmatrix}.$$

826 A computation similar to that illustrated in detail in section 3.2.1 shows that each $p_n \in \mathbb{R}^{2N}$
 827 with $n \geq 2$ is a solution of the equation

$$828 \quad [DF(p_0) - \lambda^n \text{Id}_{2N \times 2N}] p_n = S_n^N,$$

830 with S_n^N defined by

$$831 \quad S_n^N := \begin{pmatrix} a \sum_{k=1}^{n-1} p_{n-k,1}^N p_{k,1}^N & 0 \\ a \sum_{k=1}^{n-1} p_{n-k,1}^1 p_{k,1}^1 & 0 \\ \vdots & \vdots \\ a \sum_{k=1}^{n-1} p_{n-k,1}^{N-1} p_{k,1}^{N-1} & 0 \end{pmatrix}.$$

833 Again, we see that the linear system has a unique solution for all $n \geq 2$ by the assumption
 834 that the orbit is hyperbolic, as $\lambda^n \neq \lambda$ for any $n \geq 2$. Solving the system to order K leads to
 835 the polynomial approximation

$$836 \quad P_K(\theta) := \sum_{n=0}^K p_n \theta^n.$$

838 **3.2.3. Example of a two-dimensional manifold for a three-dimensional map: Stable/
 839 unstable manifolds for periodic orbits of the Lomelí map.** Consider the map $f: \mathbb{R}^3 \rightarrow \mathbb{R}^3$
 840 given by

$$841 \quad (20) \quad f(x, y, z) = \begin{pmatrix} z + Q(x, y) \\ x \\ y \end{pmatrix},$$

843 where Q is the quadratic form

$$844 \quad Q(x, y) = \alpha + \tau x + ax^2 + bxy + cy^2.$$

846 We refer to (20) as the Lomelí map. It is standard to choose parameters normalized so that
 847 $a + b + c = 1$. The Lomelí map is a normal form for quadratic volume-preserving maps with
 848 quadratic inverse. In that sense it can be thought of as a three-dimensional generalization
 849 of the planar Hénon map. The dynamics of the Lomelí map are considered in a number of
 850 studies; see, for example, [29, 53, 54, 62].

851 Now let

$$852 \quad \tilde{F}(x_1, y_1, z_1, \dots, x_N, y_N, z_N) = \begin{pmatrix} z_N + Q(x_N, y_N) \\ x_N \\ y_N \\ \vdots \\ z_1 + Q(x_1, y_1) \\ x_1 \\ y_1 \end{pmatrix}.$$

853
854 Suppose that $(p^1, \dots, p^N) \in \mathbb{R}^{3N}$ is a fixed point of F ; i.e., p^1, \dots, p^N is a periodic orbit.

855 We focus on the case which the orbit is hyperbolic with a complex conjugate pair of
856 stable/unstable eigenvalues. More precisely, assume that $Df^N(p_k)$ has a complex conjugate
857 pair of eigenvalues $\tilde{\lambda}, \bar{\tilde{\lambda}} \in \mathbb{C}$, and let $\xi^k, \bar{\xi}^k$ be an associated choice of complex conjugate
858 eigenvectors. Take λ and $\bar{\lambda}$ complex conjugates with

$$859 \quad \lambda = \sqrt[N]{\tilde{\lambda}} \quad \text{and} \quad \bar{\lambda} = \sqrt[N]{\bar{\tilde{\lambda}}}.$$

861 Of course we have again that $\lambda, \bar{\lambda}, \xi^1, \bar{\xi}^1, \dots, \xi^N, \bar{\xi}^N$ can be found by computing eigenval-
862 ues/eigenvectors of $DF(p^1, \dots, p^N)$.

863 In this case we employ complex variables and look for $P^{(k)}: \mathbb{C}^2 \rightarrow \mathbb{C}^3$ solving the invariance
864 equations

$$865 \quad \begin{aligned} f(P^{(N)}(z_1, z_2)) &= P^{(1)}(\lambda z_1, \bar{\lambda} z_2) \\ 866 \quad f(P^{(1)}(z_1, z_2)) &= P^{(2)}(\lambda z_1, \bar{\lambda} z_2) \\ &\vdots \\ 867 \quad f(P^{(N-1)}(z_1, z_2)) &= P^{(N)}(\lambda z_1, \bar{\lambda} z_2). \end{aligned}$$

869 We look for solutions in the form

$$870 \quad P^{(k)}(z_1, z_2) = \sum_{n_1=0}^{\infty} \sum_{n_2=0}^{\infty} p_{n_1, n_2}^k z_1^{n_1} z_2^{n_2}$$

872 for each $1 \leq k \leq N$, where $p_{n_1, n_2}^k \in \mathbb{C}^3$ for each $n_1, n_2 \in \mathbb{N}$. The components are expressed as
873 $p_{n_1, n_2}^k = (p_{n_1, n_2, 1}^k, p_{n_1, n_2, 2}^k, p_{n_1, n_2, 3}^k) \in \mathbb{C}^3$. We write

$$874 \quad p_0 = \begin{pmatrix} p^1 \\ \vdots \\ p^N \end{pmatrix}, \quad p_{1,0} = \begin{pmatrix} \xi^1 \\ \vdots \\ \xi^N \end{pmatrix}, \quad \text{and} \quad p_{0,1} = \begin{pmatrix} \bar{\xi}^1 \\ \vdots \\ \bar{\xi}^N \end{pmatrix},$$

876 for the zero- and first-order Taylor coefficients, and write more generally

$$877 \quad P(z_1, z_2) = \sum_{n_1=0}^{\infty} \sum_{n_2=0}^{\infty} p_{n_1, n_2} z_1^{n_1} z_2^{n_2},$$

878

879 where

$$880 \quad p_{n_1, n_2} = \begin{pmatrix} p_{n_1, n_2}^1 \\ \vdots \\ p_{n_1, n_2}^N \end{pmatrix},$$

881 noting that

$$882 \quad P^{(k)}(\lambda z_1, \bar{\lambda} z_2) = \sum_{n_1=0}^{\infty} \sum_{n_2=0}^{\infty} \lambda^{n_1} \bar{\lambda}^{n_2} p_{n_1, n_2}^{(k)} z_1^{n_1} z_2^{n_2}$$

883 and (after using the two variable Cauchy product) that

$$884 \quad f[P^{(k)}(z_1, z_2)] = \begin{pmatrix} \alpha + \sum_{n_1=0}^{\infty} \sum_{n_2=0}^{\infty} \infty \left(p_{n_1, n_2, 3}^{(k)} + \tau p_{n_1, n_2, 1}^{(k)} + q_{n_1, n_2}^{(k)} \right) z_1^{n_1} z_2^{n_2} \\ \sum_{n_1=0}^{\infty} \sum_{n_2=0}^{\infty} p_{n_1, n_2, 1}^{(k)} z_1^{n_1} z_2^{n_2} \\ \sum_{n_1=0}^{\infty} \sum_{n_2=0}^{\infty} p_{n_1, n_2, 2}^{(k)} z_1^{n_1} z_2^{n_2} \end{pmatrix},$$

885 where

$$886 \quad q_{n_1, n_2}^{(k)} = \sum_{i=0}^{n_1} \sum_{j=0}^{n_2} a p_{n_1-i, n_2-j, 1}^{(k)} p_{i, j, 1}^{(k)} + b p_{n_1-i, n_2-j, 1}^{(k)} p_{i, j, 2}^{(k)} + c p_{n_1-i, n_2-j, 2}^{(k)} p_{i, j, 2}^{(k)}.$$

887 Matching like powers for $n_1 + n_2 \geq 2$ leads to

$$888 \quad \begin{pmatrix} p_{n_1, n_2, 3}^{(N)} + \tau p_{n_1, n_2, 1}^{(N)} + q_{n_1, n_2}^{(N)} \\ p_{n_1, n_2, 1}^{(N)} \\ p_{n_1, n_2, 2}^{(N)} \end{pmatrix} = \lambda^{n_1} \bar{\lambda}^{n_2} \begin{pmatrix} p_{n_1, n_2, 1}^{(1)} \\ p_{n_1, n_2, 2}^{(1)} \\ p_{n_1, n_2, 3}^{(1)} \end{pmatrix}$$

889 and

$$890 \quad \begin{pmatrix} p_{n_1, n_2, 3}^{(k-1)} + \tau p_{n_1, n_2, 1}^{(k-1)} + q_{n_1, n_2}^{(k-1)} \\ p_{n_1, n_2, 1}^{(k-1)} \\ p_{n_1, n_2, 2}^{(k-1)} \end{pmatrix} = \lambda^{n_1} \bar{\lambda}^{n_2} \begin{pmatrix} p_{n_1, n_2, 1}^{(k)} \\ p_{n_1, n_2, 2}^{(k)} \\ p_{n_1, n_2, 3}^{(k)} \end{pmatrix}$$

891 for $2 \leq k \leq N$. Let $s_{n_1, n_2} = (S_{n_1, n_2}^{(N)}, S_{n_1, n_2}^{(1)}, \dots, S_{n_1, n_2}^{(N-1)})$ and

$$892 \quad (21) \quad S_{n_1, n_2}^{(k)} = \begin{pmatrix} \sum_{i=0}^{n_1} \sum_{j=0}^{n_2} \delta_{j, k}^{n_1, n_2} \left(a p_{n_1-i, n_2-j, 1}^{(k)} p_{i, j, 1}^{(k)} + b p_{n_1-i, n_2-j, 1}^{(k)} p_{i, j, 2}^{(k)} + c p_{n_1-i, n_2-j, 2}^{(k)} p_{i, j, 2}^{(k)} \right) \\ 0 \\ 0 \end{pmatrix},$$

893

899 where we define

$$900 \quad \delta_{j,k}^{n_1, n_2} := \begin{cases} 0 & \text{if } j = n_1 \text{ and } k = n_2, \\ 0 & \text{if } j = 0 \text{ and } k = 0, \\ 1 & \text{otherwise.} \end{cases}$$

902 Then

$$903 \quad q_{n_1, n_2}^{(k)} = 2ap_{0,0,1}^{(k)} p_{n_1, n_2, 1} + bp_{0,0,1} p_{n_1, n_2, 2} + bp_{0,0,2} p_{n_1, n_2, 1} + cp_{0,0,2} p_{n_1, n_2, 2}.$$

905 Thus, the Taylor coefficient p_{n_1, n_2} is found by solving the homological equation

$$906 \quad (22) \quad [DF(p_0) - \lambda^{n_1} \bar{\lambda}^{n_2} \text{Id}_{3N \times 3N}] p_{n_1, n_2} = S_{n_1, n_2}.$$

908 Again we remark that these are always uniquely solvable in the case under consideration,
909 namely a periodic hyperbolic saddle with a complex conjugate pair. This is because if $n_1 + n_2 \geq$
910 2, then neither

$$911 \quad \lambda^{n_1} \bar{\lambda}^{n_2} = \lambda \quad \text{nor} \quad \lambda^{n_1} \bar{\lambda}^{n_2} = \bar{\lambda}$$

913 is possible, and since the Lomelí map is volume-preserving, the third eigenvalue must have
914 opposite stability from $\lambda, \bar{\lambda}$ (i.e., the eigenvalue is unstable if they are stable or vice versa).
915 More generally a periodic orbit with a single complex conjugate pair of stable (or unstable)
916 eigenvalues cannot be resonant.

917 We write

$$918 \quad P_K(\theta) = \sum_{n=0}^K \sum_{m=0}^n p_{n-m, m} \theta_1^{n-m} \theta_2^m$$

920 to denote the polynomial approximation obtained by solving the homological equations to
921 order K .

922 *Remark 3.5 (real parameterization).* In the end, we are actually interested in the real
923 dynamics of the Lomelí map and want the real image of P . By Considering (22), we see that
924 solutions have the property

$$925 \quad p_{m_2, m_1} = \overline{p_{m_1, m_2}}.$$

927 This complex conjugate property of the coefficients of P implies that if we choose complex
928 conjugate variables

$$929 \quad z_1 = \theta + i\phi \quad \text{and} \quad z_2 = \theta - i\phi$$

931 and define the polynomial

$$932 \quad \hat{P}(\theta, \phi) = P(\theta + i\phi, \theta - i\phi),$$

934 where P has coefficients solving (22), then \hat{P} parameterizes the real local stable/unstable
935 manifolds associated with the periodic orbit.

936 **3.2.4. Example of a nonpolynomial nonlinearity: Automatic differentiation for the**
 937 **standard map.** We now consider the map $f: \mathbb{R}^2 \rightarrow \mathbb{R}^2$ given by

$$938 \quad (23) \quad f(x, y) = \begin{pmatrix} x + a \sin(y) \\ y + x + a \sin(y) \end{pmatrix},$$

939
 940 with $a \geq 0$. The map is known as the *standard map*, or the Chirikov–Taylor map, and is
 941 widely studied as a toy model of symplectic dynamics [16, 36, 58]. For example, the mapping
 942 exhibits dynamics similar to the dynamics of a Poincaré section of a periodic orbit of a two
 943 freedom Hamiltonian system restricted to an energy surface. We now derive the homological
 944 equations for the parameterization of the stable/unstable manifold of a period N orbit of
 945 the standard map. This illustrates the use of our method for a system with nonpolynomial
 946 nonlinearities.

947 Then suppose that $p^1, \dots, p^N \in \mathbb{R}^2$ are the points of a periodic orbit of least period N .
 948 Assume that the orbit is hyperbolic, and let $\xi^1, \dots, \xi^N \in \mathbb{R}^2$ and $\tilde{\lambda} \in \mathbb{R}$ denote the associated
 949 eigenvalues and eigenvectors. We let

$$950 \quad \lambda = \sqrt[N]{\tilde{\lambda}}$$

951 and look for solutions

$$952 \quad P^{(k)}(\theta) = \sum_{n=0}^{\infty} p_n^{(k)} \theta^n$$

953 of (15) in this setting. Let us write

$$954 \quad p_n^{(k)} = \begin{pmatrix} p_{n,1}^{(k)} \\ p_{n,2}^{(k)} \end{pmatrix}$$

955 for $1 \leq k \leq N$ to denote the components of $p_n^{(k)}$.

956 This difference between the present case and the examples discussed above is that the
 957 standard map has nonpolynomial nonlinearity, so that $f[P^{(k)}]$ cannot be evaluated directly
 958 using Cauchy products. Instead, we employ a technique sometimes called *automatic differen-*
 959 *tiation for Taylor series*, or simply automatic differentiation [46]. The idea is to exploit the
 960 fact that the sine and cosine functions are themselves solutions of simple differential equations.
 961 Thus, define for each $1 \leq k \leq N$ the functions $S^{(k)}, C^{(k)}$ by

$$962 \quad S^{(k)}(\theta) := \sin\left(P_2^{(k)}(\theta)\right)$$

963 and

$$964 \quad C^{(k)}(\theta) := \cos\left(P_2^{(k)}(\theta)\right)$$

965 and look for the Taylor series expansions

$$966 \quad \sum_{n=0}^{\infty} s_n^{(k)} \theta^n = S^{(k)}(\theta)$$

967

968

969

970

971

972

973 and

$$974 \quad \sum_{n=0}^{\infty} c_n^{(k)} \theta^n = C^{(k)}(\theta).$$

976 Taking derivatives, we obtain

$$977 \quad \frac{d}{d\theta} S^{(k)}(\theta) = \cos\left(P_2^{(k)}(\theta)\right) \frac{d}{d\theta} P_2^{(k)}(\theta)$$

979 and

$$980 \quad \frac{d}{d\theta} C^{(k)}(\theta) = -\sin\left(P_2^{(k)}(\theta)\right) \frac{d}{d\theta} P_2^{(k)}(\theta),$$

982 which on the level of power series give

$$983 \quad \sum_{n=0}^{\infty} (n+1) s_{n+1}^{(k)} \theta^n = \left(\sum_{n=0}^{\infty} c_n \theta^n \right) \left(\sum_{n=0}^{\infty} (n+1) p_{n,2}^{(k)} \theta^n \right)$$

$$984 \quad = \sum_{n=0}^{\infty} \sum_{j=0}^n (j+1) c_{n-j}^{(k)} p_{j+1,2}^{(k)} \theta^n,$$

985 and similarly

$$986 \quad \sum_{n=0}^{\infty} (n+1) c_{n+1}^{(k)} \theta^n = - \sum_{n=0}^{\infty} \sum_{j=0}^n (j+1) s_{n-j}^{(k)} p_{j+1,2}^{(k)} \theta^n.$$

988 Of course we have

$$989 \quad s_0^{(k)} = \sin\left(p_{0,2}^{(k)}\right) \quad \text{and} \quad c_0^{(k)} = \cos\left(p_{0,2}^{(k)}\right)$$

991 as well as

$$992 \quad s_1^{(k)} = \cos\left(p_{0,2}^{(k)}\right) p_{1,2}^{(k)} \quad \text{and} \quad c_1^{(k)} = -\sin\left(p_{0,2}^{(k)}\right) p_{1,2}^{(k)}$$

994 Matching like powers of n for $n \geq 2$ gives

$$995 \quad s_n^{(k)} = \frac{1}{n} \sum_{j=1}^n j c_{n-j}^{(k)} p_{j,2}^{(k)} = c_0^{(k)} p_{n,2}^{(k)} + \frac{1}{n} \sum_{j=1}^{n-1} j c_{n-j}^{(k)} p_{j,2}^{(k)}$$

997 and

$$998 \quad c_n^{(k)} = \frac{-1}{n} \sum_{j=1}^n j s_{n-j}^{(k)} p_{j,2}^{(k)} = -s_0^{(k)} p_{j,2}^{(k)} - \frac{1}{n} \sum_{j=1}^{n-1} j s_{n-j}^{(k)} p_{j,2}^{(k)}.$$

1000

1001 Now let

$$1002 \quad P(\theta) = \begin{pmatrix} P^{(1)}(\theta) \\ \vdots \\ P^{(N)}(\theta) \end{pmatrix}.$$

1004 Then

$$1005 \quad P(\lambda\theta) = \sum_{n=0}^{\infty} \lambda^n p_n \theta^n,$$

1007 while

$$1008 \quad f[P^{(k)}(\theta)] = \begin{pmatrix} P_1^k(\theta) + a \sin(P_2^{(k)}(\theta)) \\ P_1^k(\theta) + P_2^{(k)}(\theta) + a \sin(P_2^{(k)}(\theta)) \end{pmatrix}$$

$$1009 \quad = \sum_{n=0}^{\infty} \begin{pmatrix} p_{n,1}^{(k)} + a s_n^{(k)} \\ p_{n,1}^{(k)} + p_{n,2}^{(k)} + a s_n^{(k)} \end{pmatrix} \theta^n.$$

1010 The n th coefficient of this power series is

$$1011 \quad \begin{pmatrix} p_{n,1}^{(k)} + a s_n^{(k)} \\ p_{n,1}^{(k)} + p_{n,2}^{(k)} + a s_n^{(k)} \end{pmatrix} = \begin{pmatrix} p_{n,1}^{(k)} + a c_0^{(k)} p_{n,2}^{(k)} + \frac{a}{n} \sum_{j=1}^{n-1} j c_{n-j}^{(k)} p_{j,2}^{(k)} \\ p_{n,1}^{(k)} + p_{n,2}^{(k)} + a c_0^{(k)} p_{n,2}^{(k)} + \frac{a}{n} \sum_{j=1}^{n-1} j c_{n-j}^{(k)} p_{j,2}^{(k)} \end{pmatrix}$$

$$1012 \quad = \begin{pmatrix} 1 & a \cos(p_{0,2}^{(k)}) \\ 1 & 1 + a \cos(p_{0,2}^{(k)}) \end{pmatrix} \begin{bmatrix} p_{n,1}^{(k)} \\ p_{n,2}^{(k)} \end{bmatrix} + \begin{bmatrix} \frac{a}{n} \sum_{j=1}^{n-1} j c_{n-j}^{(k)} p_{j,2}^{(k)} \\ \frac{a}{n} \sum_{j=1}^{n-1} j c_{n-j}^{(k)} p_{j,2}^{(k)} \end{bmatrix}.$$

1013 Matching like powers in the invariance equations gives that the homological equation has
1014 the desired form

$$1015 \quad (24) \quad [DF(p_0) - \lambda^n \text{Id}_{2N \times 2N}] p_n = \Sigma_n$$

1017 for $n \geq 2$, where Σ_n is given by

$$1018 \quad \Sigma_n = \begin{pmatrix} \Sigma_n^{(N)} \\ \Sigma_n^{(1)} \\ \vdots \\ \Sigma_n^{(N-1)} \end{pmatrix}$$

1019

1020 and

$$1021 \quad \Sigma_n^{(k)} = \begin{pmatrix} \frac{-a}{n} \sum_{j=1}^{n-1} j c_{n-j}^{(k)} p_{n,2}^{(k)} \\ \frac{-a}{n} \sum_{j=1}^{n-1} j c_{n-j}^{(k)} p_{n,2}^{(k)} \end{pmatrix}$$

1022
1023 for $1 \leq k \leq N$.

1024 Note that once $(p_{n,1}^{(k)}, p_{n,2}^{(k)})$ are computed as the components of the solution of the
1025 n -th homological equation (24), $s_{n+1}^{(k)}$ and $c_{n+1}^{(k)}$ are computed and stored for use in the solution
1026 of the $(n+1)$ th homological equation. The automatic differentiation scheme just described
1027 allows us to compute the power series coefficients of the composition $\sin(P_2^{(k)}(\theta))$ for the cost
1028 of two Cauchy products. However, this approach requires us to store the coefficients $s_n^{(k)}$ and
1029 $c_n^{(k)}$ throughout the computation.

1030 **3.2.5. Further remarks on automatic differentiation: Nonlinearities given by the ele-**
1031 **mentary functions of mathematical physics.** The procedure discussed in section 3.2.4 can be
1032 made quite general. We elaborate briefly below, but the interested reader should also consult
1033 [11, 38, 45, 46, 74] for a more complete discussion. In particular, the first reference describes
1034 a general algorithmic framework for manipulation of power series in nonlinear problems. The
1035 idea is that the *elementary functions of mathematical physics* comprising the nonlinear terms
1036 in many applied problems are themselves solutions of simple differential equations. This lets
1037 us extend the ideas exploited in section 3.2.4 to many other situations.

1038 To formalize the discussion, suppose

$$1039 \quad P(\theta) = \sum_{n=0}^{\infty} p_n \theta^n, \quad Q(\theta) = \sum_{n=0}^{\infty} q_n \theta^n, \quad R(\theta) = \sum_{n=0}^{\infty} r_n \theta^n$$

1041 are power series with $p_n, q_n, r_n \in \mathbb{C}$ for $n \geq 0$. The following lists several useful results for
1042 some common nonlinear functions.

1043 • **Addition:** If $R(\theta) = P(\theta) + Q(\theta)$, then

$$1044 \quad r_n = p_n + q_n.$$

1046 • **Multiplication:** If $R(\theta) = P(\theta)Q(\theta)$, then

$$1047 \quad r_n = \sum_{k=0}^n p_{n-k} q_k.$$

1049 • **Division:** If $R(\theta) = P(\theta)/Q(\theta)$, then

$$1050 \quad r_n = \frac{1}{q_0} \left(p_n - \sum_{k=1}^n r_{n-k} q_k \right).$$

1051

- 1052 • **Powers:** If $\alpha \in \mathbb{C}$ and $R(\theta) = P(\theta)^\alpha$, then

$$1053 \quad r_n = \frac{1}{np_0} \sum_{k=0}^{n-1} (n\alpha - k(\alpha + 1))p_{n-k}r_k.$$

- 1054
- 1055 • **The natural exponential:** If $R(\theta) = e^{P(\theta)}$, then

$$1056 \quad r_n = \frac{1}{n} \sum_{k=0}^{n-1} (n - k)p_{n-k}r_k.$$

- 1057
- 1058 • **The natural logarithm:** If $R(\theta) = \log P(\theta)$, then

$$1059 \quad r_n = \frac{1}{p_0} \left(p_n - \frac{1}{n} \sum_{k=1}^{n-1} (n - k)r_{n-k}p_k \right).$$

- 1060
- 1061 • **Sine and cosine:** If $R(\theta) = \sin(P(\theta))$ and $Q(\theta) = \cos(P(\theta))$, then

$$1062 \quad r_n = \frac{-1}{n} \sum_{k=1}^n kq_{n-k}p_k$$

1063

1064 and

$$1065 \quad q_n = \frac{1}{n} \sum_{k=1}^n kr_{n-k}p_k.$$

1066

1067 See [45] for proofs. Using these formulas, one could apply the techniques of the present work
 1068 to any map with nonlinearities given by the elementary functions. Moreover similar recursion
 1069 can be obtained for other elementary functions such as Bessel functions, elliptic integrals,
 1070 etc. Moreover techniques of automatic differentiation extend to functions of several complex
 1071 variables via the *radial gradient* method discussed in section 2.3.2 of [39].

1072 **4. Numerical implementation and example computations.** The results of the previous
 1073 section lead to numerical procedures as follows: for a period N orbit, find the m stable (or
 1074 unstable) eigenvalues, and compute associated eigenvectors. This latter step involves an arbi-
 1075 trary choice of the scalings. Suppose that polynomial approximation to order $K \geq 2$ is desired
 1076 and that the eigenvalues are nonresonant. Then solve the homological equations in increasing
 1077 order 2, 3, ..., up to K . This leads to a collection of polynomials $P_K^1, \dots, P_K^N: \mathbb{R}^m \rightarrow \mathbb{R}^M$.

1078 The K th order polynomials $P_K^j: \mathbb{R}^m \rightarrow \mathbb{R}^M$ for $1 \leq j \leq m$ are defined and analytic on
 1079 all of \mathbb{R}^m . Of course we cannot expect the associated truncation error to be small on all
 1080 \mathbb{R}^m , and we always restrict ourselves to a *numerical domain* on which the approximation is
 1081 reasonable. Recall that by Claim 3 from section 3.1, we are free to fix the numerical domain
 1082 as $B_1^m(0) \subset \mathbb{R}^m$ and choose the scalings of the eigenvectors so that the polynomial is well
 1083 behaved on this domain. Evaluating the polynomials only for variables smaller than one leads
 1084 to numerically stable results.

1085 The only remaining question is how to choose the scalings of the eigenvectors. We would
 1086 like to choose these scalings as large as possible so as to parameterize large regions of the
 1087 stable/unstable manifold and hence learn as much as possible about the manifolds far from
 1088 the periodic orbit. On the other hand, we also want the approximation to be reliable on
 1089 $B_1^m(0)$. We quantify the notion of reliability by defining the *a posteriori error* associated with
 1090 the polynomials P_K^1, \dots, P_K^N as the positive number

$$1091 \quad (25) \quad \varepsilon_K := \max_{1 \leq j \leq M} \left(\sup_{\theta \in B_1^m(0)} \left\| f(P_K^j(\theta_1, \dots, \theta_m)) - P_K^{j+1}(\lambda_1 \theta_1, \dots, \lambda_m \theta_m) \right\| \right),$$

1093 where we let $P_K^{N+1}(\theta) = P_K^1(\theta)$, i.e., impose periodicity. If the a posteriori error associ-
 1094 ated with P_K is small, this means that the conjugacy is approximately satisfied, and we are
 1095 reasonable confident (but not certain) that our approximation is good.

1096 The following describes an algorithm which, given an approximation order K and a desired
 1097 numerical tolerance ϵ_{tol} , adaptively rescales the eigenvectors until the scalings are
 1098 as large as possible without exceeding the numerical tolerance. The discussion in the next
 1099 section sheds further light on the procedure.

- 1100 • **Inputs:** Choose a period N orbit and compute its eigenvectors scaled initially to
 1101 length one. Fix a tolerance ϵ_{tol} and a polynomial order of approximation K .
- 1102 • *Step 1:* Compute the Taylor coefficients of P^1, \dots, P^N by solving the homological
 1103 equations to order K .
- 1104 • *Step 2:* Evaluate the a posteriori error ε_K defined in (25) (or as discussed in Remark
 1105 4.1 below).
- 1106 • *Step 3:* If $\varepsilon_K < \epsilon_{\text{tol}}$, then the scale is increased and Step 2 is repeated. If $\epsilon_{\text{tol}} \leq \varepsilon_K$,
 1107 then the scale is decreased.
- 1108 Repeat until ε_K is below but within (for example) 95% of ϵ_{tol} .

1109 *Remark 4.1 (analytic norms).* In practice we can obtain efficient numerical bounds on the
 1110 a posteriori error by computing only on the level of the coefficients. In fact if $g: \mathbb{C}^m \rightarrow \mathbb{C}$ is
 1111 analytic on the unit poly-disk

$$1112 \quad D_1^m(0) := \left\{ z = (z_1, \dots, z_m) \in \mathbb{C}^m \mid \max_{1 \leq j \leq m} |z_j| < 1 \right\},$$

1114 then by the maximum modulus principle and the triangle inequality, we have

$$1115 \quad \sup_{\theta \in B_1^m(0)} |g(\theta)| \leq \sup_{z \in \partial D_1^m(0)} |g(z)| \leq \sum_{n=0}^{\infty} |g_n|,$$

1117 where $g_n \in \mathbb{C}$ are the power series coefficients of g . Note that the inequality above holds even
 1118 when one or more of the quantities are infinite. The final quantity on the right is an ℓ^1 norm
 1119 on the Taylor coefficient, sometimes referred to as an analytic norm.

1120 Consider the a posteriori error in (25) in the case that f is a polynomial. Then $f(P_K^j(\theta_1,$
 1121 $\dots, \theta_m)$ and $P_K^{j+1}(\lambda_1 \theta_1, \dots, \lambda_m \theta_m)$ are both polynomials so that

$$f(P_K^j(\theta_1, \dots, \theta_m)) - P_K^{j+1}(\lambda_1\theta_1, \dots, \lambda_m\theta_m) = \sum_{|\alpha|=0}^{\hat{K}} e_\alpha \theta^\alpha$$

for some $e_\alpha \in \mathbb{R}^M$. Moreover the coefficients e_α are computed at the cost of an evaluation of f (on a polynomial). Then we can bound the a posteriori error by

$$\varepsilon_K \leq \sum_{|\alpha|=0}^{\hat{K}} \|e_\alpha\|.$$

If P_K^1, \dots, P_K^N are good approximations, then the coefficients e_α will be small, and this provides a good bound. If f is not a polynomial, then we must include a Taylor remainder bound in the estimates above.

4.1. A detailed numerical example: Eigenvector scalings and the size of the local manifold embedding. Returning to the Hénon map as defined in (7), consider the classic parameter values of $a = 1.4$ and $b = 0.3$, and note that the points

$$p_0 = \begin{pmatrix} -0.475800051175056 \\ 0.292740015352517 \end{pmatrix} \quad \text{and} \quad q_0 = \begin{pmatrix} 0.975800051175056 \\ -0.142740015352517 \end{pmatrix}$$

have $f(p_0) = q_0$ and $f(q_0) = p_0$; i.e., they provide a period two orbit. We check that $Df^2(p_0)$ has an unstable eigenvalue of $\tilde{\lambda} = -3.010100667740269$ (of course this is also an unstable eigenvalue of $Df^2(q_0)$) and choose associated eigenvectors

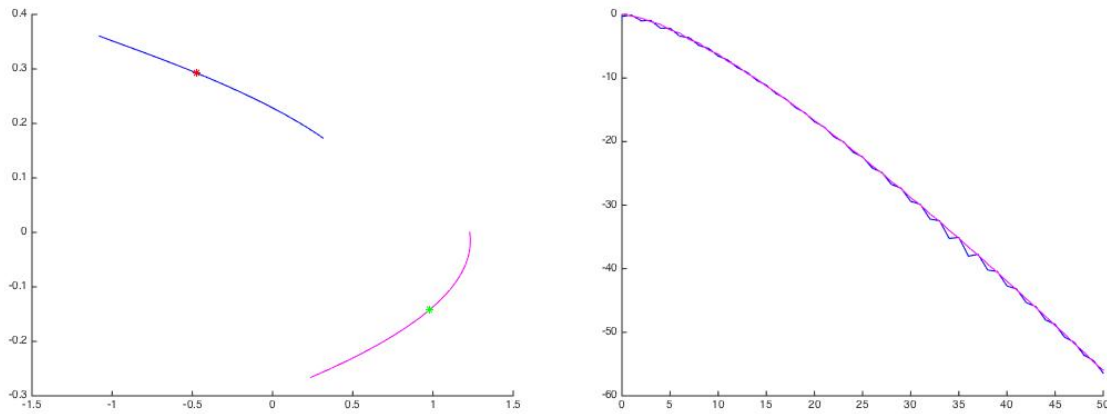
$$\tilde{\xi} = \begin{pmatrix} 0.807903584327622 \\ -0.097548838689916 \end{pmatrix} \quad \text{and} \quad \tilde{\eta} = \begin{pmatrix} -0.564145799517692 \\ -0.139698029289516 \end{pmatrix}.$$

Taking $\lambda = \sqrt{\tilde{\lambda}} = 1.734964169007611i$, we have the necessary ingredients to solve the homological equations (19) and compute polynomial charts $P(\theta)$ and $Q(\theta)$ for the local unstable manifolds of the period two orbit to any desired finite order of approximation K .

Suppose (somewhat arbitrarily) that, given the choice of eigenvectors above, we compute the parameterizations to order $K = 50$. We evaluate the resulting polynomials P^K and Q^K on the unit domain $\theta \in [-1, 1]$ and obtain the approximations illustrated in the left frame of Figure 4. Now we make several remarks.

- The simultaneous computation of the 51 two-dimensional Taylor coefficients $p_0, \dots, p_{50}, q_0, \dots, q_{50} \in \mathbb{C}^2$ of P^K and Q^K (i.e., solution of the homological equations to order K) takes 0.004 seconds using MATLAB on a Mac Pro with a 3.7 GHz quad-core Intel Xenon E5 processor. (All the computation times discussed in the paper are attached to this desktop.)
- Checking the conjugacy for each of the two manifolds at 500 uniformly spaced sample points in $[-1, 1]$ yields an a posteriori error estimate of $\epsilon = 1.33 \times 10^{-15}$.
- The image of P^K (blue curve in the left frame of Figure 4) has arc length

$$\int_{-1}^1 \sqrt{\left(\frac{d}{d\theta} P_1^K(\theta)\right)^2 + \left(\frac{d}{d\theta} P_2^K(\theta)\right)^2} d\theta \approx 1.4.$$



1144 **Figure 4.** *Parameterized unstable manifold of a period two orbit of the Hénon map: polynomial approxi-*
 1145 *mation to order $K = 50$ using an eigenvector of unit length. The resulting error is on the order of 10^{-15} . Left:*
 1146 *the top-left (blue) curve is the manifold attached to p_0 , and the bottom-right (magenta) curve is the manifold*
 1147 *attached to q_0 . Each curve is the image of the unit interval, and each has arc length approximately 1.4. Right:*
 1148 *base 10 logarithm of the Taylor coefficients as a function of order. Each Taylor coefficient is a vector with two*
 1149 *components, and we plot only the log of the norm. Colors in the right frame match the conventions in the left*
 1150 *frame. Coefficient computation takes 0.004 seconds.*

1165 Note that since the parameterizations are given by polynomials, the arc length in-
 1166 tegrals can be evaluated almost exactly using a power series method. Only com-
 1167 puting the square root of a power series—using the powers law of section 3.2.5 with
 1168 $\alpha = 1/2$ —requires truncation. The arc length for Q^K (magenta curve in the left frame
 1169 of Figure 4) is also approximately 1.4.

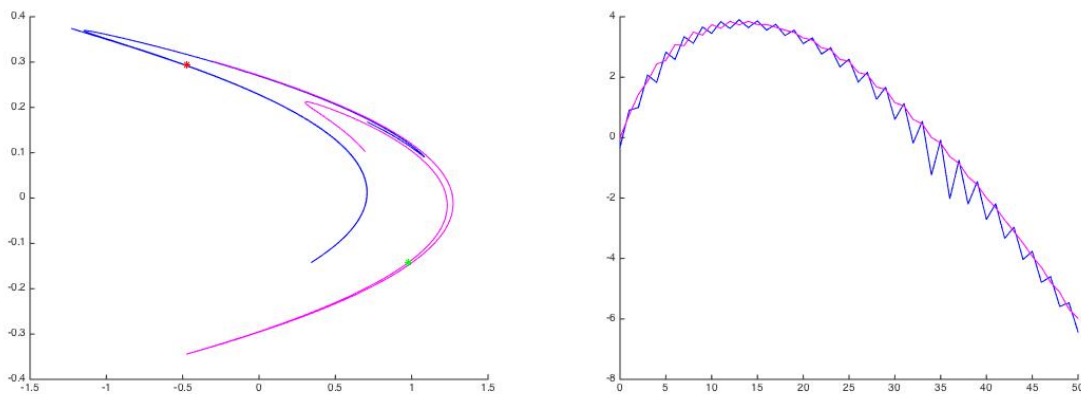
- 1170 • The logarithm base 10 of the magnitude of the Taylor coefficients is plotted versus
 1171 the order of the coefficient in the right frame of Figure 4. The coefficients decay
 1172 exponentially fast, and the coefficients of order 50 have magnitude 10^{-60} .

1173 A closer look at the right frame of Figure 4 suggests that the coefficients of the param-
 1174 eterization are decaying too fast to be numerically significant after an order of about $K = 25$,
 1175 (For $n \geq 25$, the magnitude of the Taylor coefficients of both polynomials is below 10^{-16} , i.e.,
 1176 below double precision machine epsilon). It is therefore reasonable to rescale the eigenvector
 1177 to get a slower decay rate. Keeping the same numerical domain of $[-1, 1]$, we should expect
 1178 the result to parameterize a larger section of the local unstable manifold.

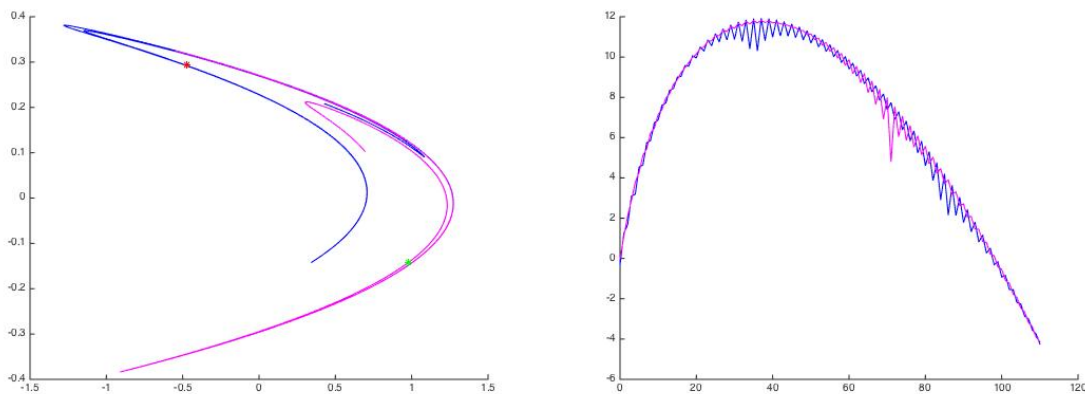
1185 Running the computations a second time, keeping $K = 50$, and taking

$$1186 \quad p_1 = 10\tilde{\xi} \quad \text{and} \quad q_1 = 10\tilde{\eta}$$

1188 results in the parameterizations illustrated in Figure 5. Again, the computation takes 0.004
 1189 seconds and results in a conjugacy error on the order of $\epsilon = 10^{-7}$. However, the arc length
 1190 of the manifolds is now about 7.3. The resulting local unstable manifold parameterizations
 1191 suggest a substantial portion of the Hénon attractor, as seen in the left frame of Figure 5.
 1192 Note that in this example the Taylor coefficients initially grow, reaching a maximum length
 1193 of almost 10^4 before the exponential decay kicks in. The order $N = 50$ coefficients have
 1194 magnitude approximately 10^{-7} , which is roughly the magnitude of the conjugacy error.



1179 **Figure 5.** Rescaled local parameterizations: polynomial approximation to order $K = 50$ using an eigenvector
 1180 of length 10. The resulting error is on the order of 10^{-7} . New curves have arc length approximately 7.3. Color
 1181 conventions are as in Figure 4. Coefficient computation takes 0.004 seconds.



1182 **Figure 6.** Rescaled local parameterizations: polynomial approximation to order $N = 110$ using an eigenvector
 1183 of length 22. The resulting error is on the order of 10^{-4} . New curves have arc length approximately 12.1.
 1184 Color conventions are as in Figure 4. Coefficient computation takes 0.0085 seconds.

1195 Indeed, if we keep this scaling factor of 10 but compute the manifolds to order $N = 60$,
 1196 then the resulting manifolds have the same length and look exactly like the parameterizations
 1197 illustrated in the left frame of Figure 5. But the $N = 60$ coefficient is on the order of 10^{-12}
 1198 in magnitude, and the resulting conjugacy error is on the order of 10^{-12} .

1199 We remark that while increasing the order of the computation past $N = 60$ does lead
 1200 to smaller coefficients, it does not further improve the conjugacy error. But it is easy to see
 1201 why. Note that the largest polynomial coefficient is on the order of 10^4 , so that the smallest
 1202 numerically significant coefficients are those of order 10^{-12} (a 16-digit spread). To obtain
 1203 more accurate results we would have to use extended precision computations.

1204 Figure 6 illustrates a final result, which seems to be near the limit of what can be done
 1205 in this example using only double precision arithmetic. The local parameterizations are

1206 computed to polynomial order $N = 110$, with the initial eigenvectors scaled by a factor of 22.
 1207 Each curve has arc length roughly 12.1, and the computation takes roughly 0.0085 seconds.
 1208 The Conjugacy error is $\epsilon = 6.9 \times 10^{-4}$, and the resulting local manifold parameterizations
 1209 uncover even more of the Hénon attractor. However, increasing the eigenvector scaling further
 1210 results in polynomial approximations which diverge visibly.

1211 *Remark 4.2 (numerical implementation).* The interested reader can reproduce these results
 1212 by running the program

1213 `henonPer2Ex1_paper.m`

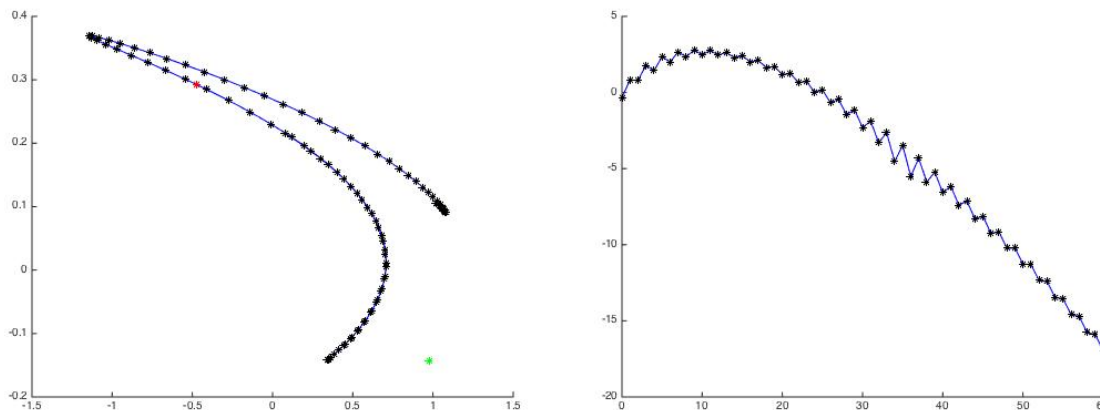
1214 which is available for free download from the authors' webpage for the preprint version of this
 1215 paper [34]. By changing only the variables `N` and `scale`, one obtains any of the results above.
 1216 The interested reader is invited to experiment with these computations.

1217 **4.2. Comparison with the naive approach.** The computational advantages of the
 1218 multiple-shooting parameterization method developed in the present work are seen clearly
 1219 when we repeat the computation of section 4.1 using the naive approach. More precisely, we
 1220 compute the parameterization of the local unstable manifold associated with the fixed point
 1221 p_0 of the composition map $f \circ f = g$, where g is as given in (8).

1222 Taking the approximation order $K = 60$ and iteratively solving the homological equations
 1223 developed in section 2.3 results in a polynomial approximation that we denote by R^N . We
 1224 compare this with our earlier results for the same manifold, already reported in Figure 5.
 1225 Carefully choosing the scaling of the eigenvector in the computation of R^N (scaling it to
 1226 6.512 where the eigenvector in the computation of P^N was scaled to 8) provides the results
 1227 illustrated in Figure 7. The Figure makes clear the virtue of the carefully chosen scaling: we
 1228 obtain almost exactly the same local parameterization of the unstable manifold that we had
 1229 before (“same” in the sense of both the embedding in phase space and the Taylor coefficient
 1230 decay). That there exists such a choice of scaling is not a surprise: the two methods compute
 1231 the same manifold.

1232 However, the Naive computation takes about 0.035 seconds—or almost a factor of five
 1233 times as long as the computation using the multiple shooting approach—after which we obtain
 1234 only one of the two manifolds computed in section 4.1. Computing both manifolds takes 10
 1235 times as long as the multiple shooting approach. In addition, the conjugacy error is an order
 1236 of magnitude worse than the multiple shooting case.

1237 The poorer run time results from the need to compute the triple and quadruple Cauchy
 1238 products appearing in the composition map (composition of the quadratic Hénon map with
 1239 itself). Indeed, a more telling comparison between the two methods is to count floating point
 1240 operations in the evaluation of the right-hand sides of the respective homological equations.
 1241 Recalling (19), we see that the right-hand side of the homological equation for the multiple-
 1242 shooting method requires evaluation of only two quadratic Cauchy products, while by (12),
 1243 the right-hand side of the homological equation for the composition approach requires two
 1244 quadratic Cauchy products as well as a cubic and a quartic evaluation. For the computations
 1245 illustrated in Figure 7, evaluating the right-hand side of the homological equations in the



1232 **Figure 7.** *Composition versus multiple shooting: unstable manifold of p_0 computed two ways. Blue curve*
 1233 *corresponds to the parameterization computed using multiple shooting. Computational parameters are the same*
 1234 *as reported in Figure 5. The black stars illustrate the same manifold, computed as the unstable manifold of a*
 1235 *fixed point of the composition map. The results look identical, but the composition approach takes five times*
 1236 *as long to compute and requires more than 300 times as many floating point operations. The error using the*
 1237 *composition approach is more than an order of magnitude worse.*

1252 naive approach is more than 300 times as expensive to compute than the right-hand side for
 1253 the multiple-shooting parameterization method.

1254 The interested reader can repeat these computations by running the program

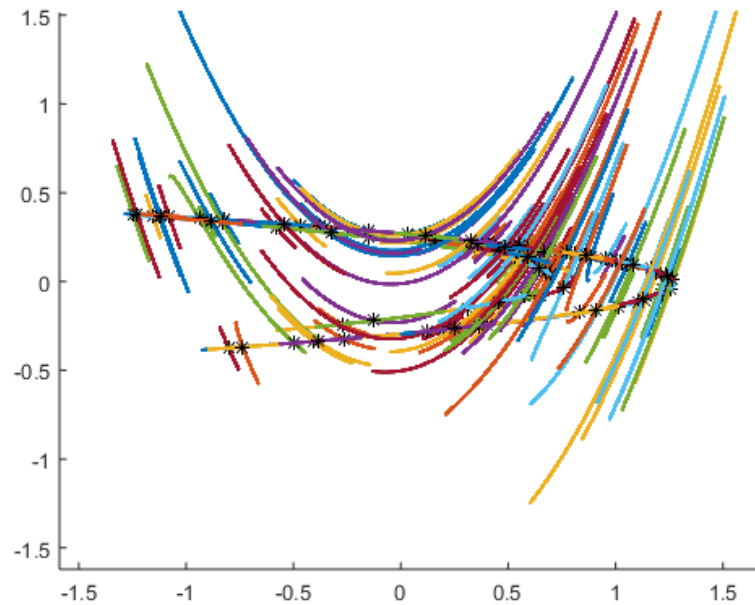
1255 `henonPer2_withComp.m`.

1256 We remark that on many laptop and desktop computers (less powerful than the Mac Pro)
 1257 the multiple-shooting method over performs the naive method by an even greater factor than
 1258 reported above.

1262 **4.3. Long periodic orbits for the Hénon map.** One strength of our algorithm is that
 1263 it applies to periods much higher than two. Figure 8 illustrates the results of our procedure
 1264 applied to a single orbit of period $M = 95$ for the Hénon map with the classic parameters
 1265 $a = 1.4$ and $b = 0.3$. The 2×95 parameterization functions are approximated to polynomial
 1266 order $M = 50$, and we employ the adaptive rescaling algorithm with a desired tolerance of
 1267 $\epsilon_{\text{tol}} = 10^{-14}$. The algorithm results in an eigenvector scaling of $s = 5.37$ for the stable and
 1268 $s = 2.74$ for the unstable manifold.

1269 *Remark 4.3 (finding orbits of long period).* We find periodic orbits (long or otherwise) for
 1270 the Hénon map as follows. We pick any point “near” the attractor (say $x = 0, y = 1$) and
 1271 iterate a large number of times (say $K = 10^5$ or more). Ignoring the first, say 100, points on
 1272 the resulting orbit segment, we have a collection of points near the attractor. We now search
 1273 this collection for orbits which are approximately period M for every $2 \leq M \leq M_{\text{max}}$. For
 1274 the Hénon map, we typically take $M_{\text{max}} < 100$.

1275 When we find an orbit segment which is approximately period M , we run a Newton
 1276 method to obtain a better orbit. We also check that the orbit we obtain has not already been

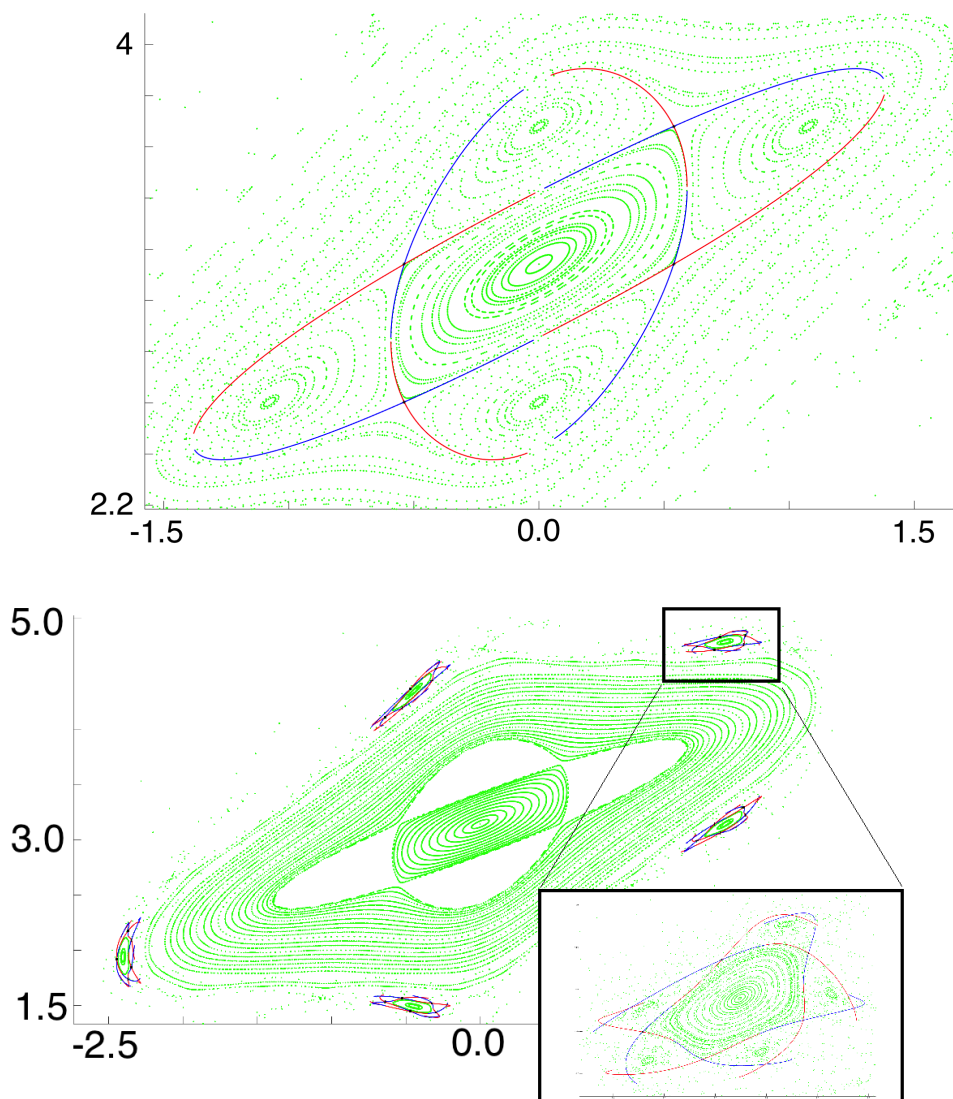


1259 **Figure 8.** *Manifolds attached to a period 95 orbit for the Hénon map: classic parameter values, approx-*
 1260 *imation order $N = 50$, and eigenvectors with optimal scaling. A posteriori error held below 10^{-14} . Unstable*
 1261 *manifolds are tangent to the attractors, and stable manifolds are normal. Colors are chosen at random.*

1277 found. If the orbit is new, that is, if M is the least period of the orbit, then we add it to
 1278 our list. This is a typical search procedure based on the notion that the dynamics on the
 1279 attractor are uniquely ergodic; hence a single long orbit should convey the same information
 1280 as sampling “uniformly” over the attractor. The procedure just described was also used to
 1281 find the orbits discussed in Remark 1.2 and illustrated in Figure 1.

1288 **4.4. Long periodic orbits in the standard map.** In this section we consider several
 1289 example results for the standard map given by (23) with $a = 2.1$, i.e., far from the inte-
 1290 grable/perturbative case. Recall that this map has transcendental nonlinearity given by the
 1291 sine function. Once we choose a periodic orbit of period M , we compute the Taylor coef-
 1292 ficients by solving the homological equations given by (24). For example, the top frame of
 1293 Figure 9 illustrates the local unstable manifolds attached to a period four point approximated
 1294 to polynomial order $N = 200$. The eigenvector is scaled to $s = 1.6$.

1295 The bottom frame of Figure 9 illustrates the stable/unstable manifolds attached to a
 1296 period 25 orbit of the standard map, again approximated to polynomial order $N = 200$.
 1297 The stable and unstable manifolds are scaled by $s = 0.95$ and $s = 0.98$, respectively. The
 1298 inlay in the figure “zooms in” on one of the KAM islands (or secondary tori) surrounding the
 1299 primary family of invariant circles in the standard map. This island shows yet another layer
 1300 of islands (or tertiary tori), and our period 25 orbit is the hyperbolic “twin” of the (presumed)
 1301 period 25 elliptic orbit in the center of the tertiary tori. The local stable/unstable manifolds
 1302 parameterized here already show homoclinic intersections.



1282 **Figure 9.** The standard map with $a = 2.1$: elliptic island near the fixed point at $(0, \pi)$. The green points
 1283 illustrate the dynamics of “typical orbits” and are obtained by simply iterating a large number of sample points.
 1284 Viewing the hyperbolic dynamics requires a more deliberate approach. Top: local stable and unstable manifolds
 1285 attached to a period four orbit. Bottom: local stable and unstable manifolds attached to a period 25 orbit. Inlay
 1286 zooms in around a secondary torus and illustrates homoclinic intersection points. Unstable manifolds are blue
 1287 and stable manifolds are red.

1303 The interested reader can repeat these computations by running the programs

1304 `standardMapPaperEx_per4.m`

1305 and

1306 `standardMapPaperEx_per25.m`.

1307 *Remark 4.4 (finding long periodic orbits for the standard map).* The standard map is an
 1308 area preserving map, and hence it has no nontrivial attractor. The full map is not uniquely
 1309 ergodic, and the strategy described in Remark 4.3 will not work. Moreover, simply sampling
 1310 the phase space can be misleading, as there are many invariant circles which will be hard to
 1311 distinguish from long periodic orbits numerically.

1312 The orbits in the examples above are found by “eyeballing” the phase space portrait and
 1313 looking for interesting features. For example, looking only at the green points in Figure 9, we
 1314 see that the dominant feature is the period four KAM islands around the primary family of
 1315 circles about the origin.

1316 Standard results for area-preserving maps tell us to expect an elliptic period four orbit
 1317 in the middle of these islands, and also that the elliptic period four point should have an
 1318 associated twin, that is, there should be a hyperbolic period four orbit nearby. A simple
 1319 inspection of the picture suggests that one point near this orbit is $x = -0.5$, $y = 2.5$. We
 1320 run a Newton method with this as the initial condition and obtain the hyperbolic period four
 1321 point accurate to machine precision. Computing the eigenvectors and solving the homological
 1322 equations is straightforward. The initial guess for the period 25 orbit was obtained in precisely
 1323 the same manner.

1324 **4.5. Period four vortex bubble in the Lomelí map.** From the planar examples mentioned
 1325 in the previous sections, one can learn a great deal about the dynamics of the system simply
 1326 by phase space sampling. For example, iterating almost any initial point in the plane for long
 1327 enough under the Hénon map yields the familiar picture of the attractor. Similarly, the green
 1328 points in Figures 9 give a reasonable impression of the dynamics in the standard map for
 1329 $a = 2.1$.

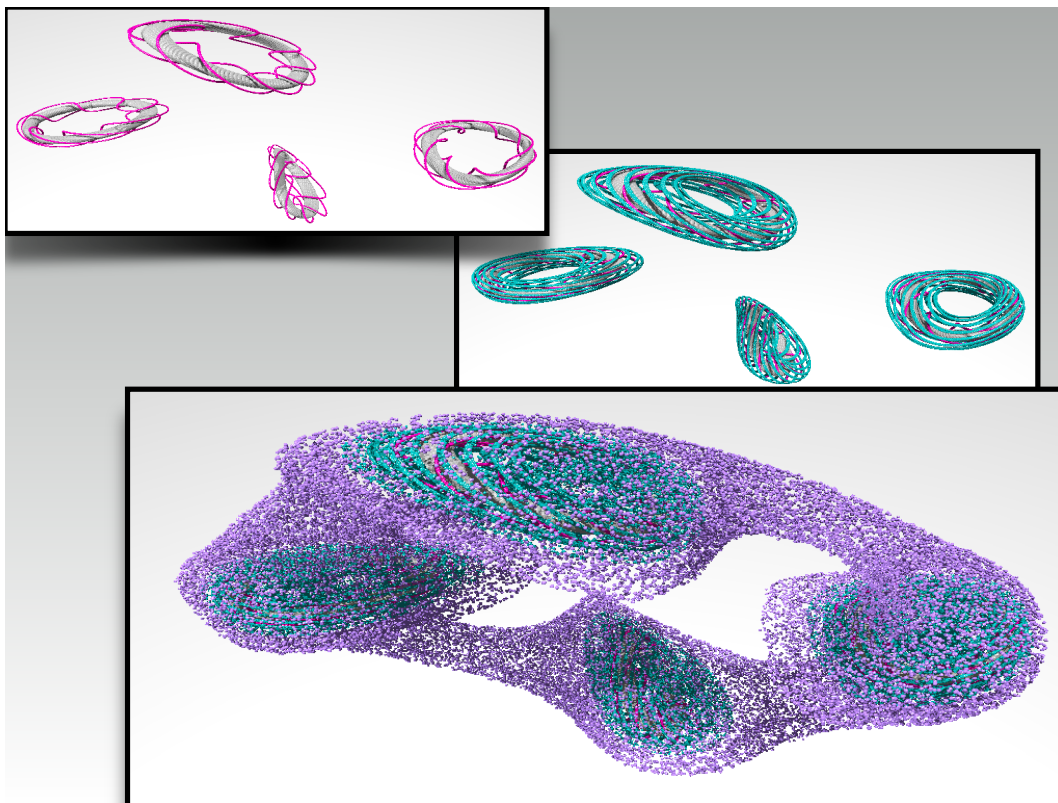
1330 For dissipative maps of \mathbb{R}^3 , things are not so different. Such maps typically have attractors,
 1331 and simply iterating a collection of points provides a good picture of the dynamics. For
 1332 volume-preserving maps of \mathbb{R}^3 , the situation is somewhat less clear.

1333 Consider, for example, the Lomelí map given by (20). Plotting a typical bounded orbit of
 1334 the system leads to an amorphous blob. And plotting many such orbits results in a “thick”
 1335 point cloud that may tell us very little. The system, however, does admit many invariant tori.

1336 Figure 10, for example, illustrates a number of orbits for the system with parameters
 1337 $a = 0.5$, $b = -0.5$, $c = 1$, $\tau = 1.333333333$, and $\alpha = 0.3444444444$. These orbits illustrate
 1338 some period four invariant tori, secondary period four tori (or invariant circles?) about these,
 1339 and finally a single invariant torus enclosing the entire structure. For each object, we are
 1340 simply iterating a single point, which is presumably near the invariant torus or circle, and we
 1341 do not have a parameterization of the tori.

1342 Moreover these orbits are not “typical”: rather, they were identified by eye as “interesting”
 1343 results from a rather larger sampling of phase space. Such a search is both time consuming and
 1344 ad hoc. Nevertheless it yields some interesting period four structures. The reader interested
 1345 in the dynamics of the Lomelí map may want to review the works of [15, 29, 53, 54, 62, 64].
 1346 Indeed, the period four tori discussed here are also seen in [54].

1356 The strategy of simply iterating points and examining the results for structure will not
 1357 directly tell us anything about hyperbolic objects. However, based on these results we can



1347 **Figure 10.** *Quasi-periodic invariant objects for the Lomelí map: Top left: period four invariant tori*
 1348 *encircled by invariant circles. Middle right: same tori with longer invariant circles. Bottom: period one*
 1349 *invariant torus encasing the period four structure. All of these invariant structures were located by phase space*
 1350 *sampling.*

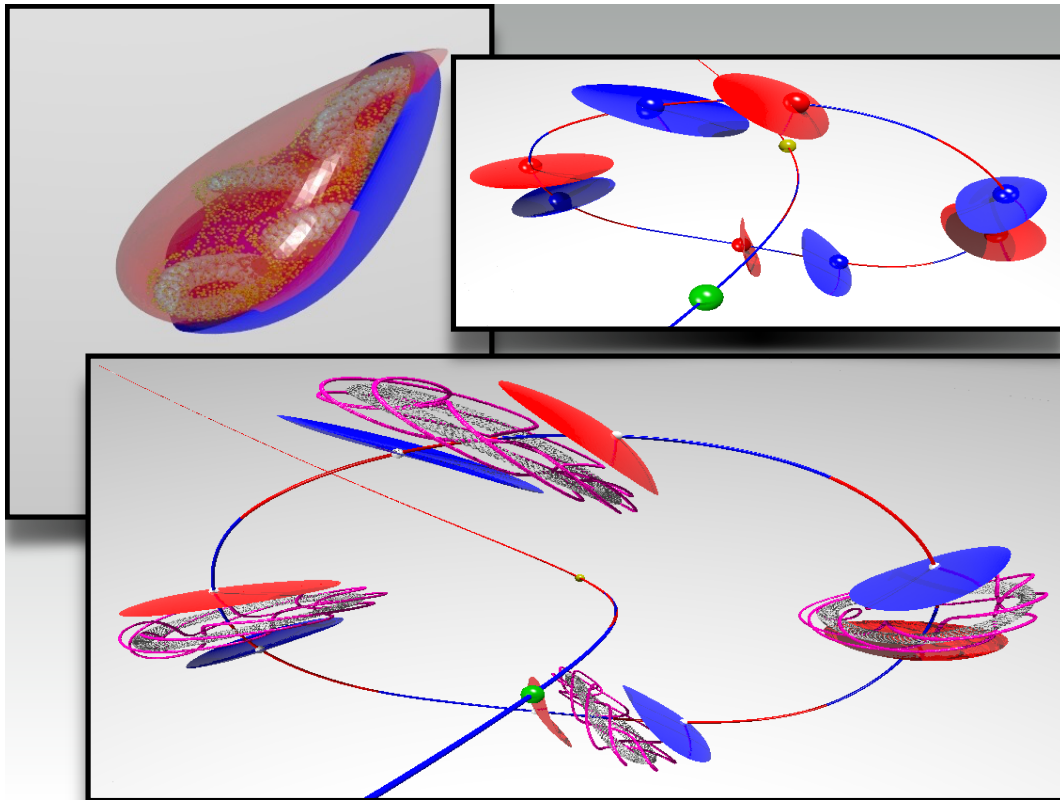
1358 *guess* that there should be a pair of hyperbolic period four points near the top and bottom of
 1359 the opening of the period four torus. Similarly, we can guess (or work out directly by hand)
 1360 that there are a pair of fixed points near the top and bottom of the opening of the larger
 1361 surrounding torus.

1362 Once we have located the period four points (or fixed points), it is a simple procedure
 1363 to compute the corresponding eigenvectors and solve the homological equations for the one-
 1364 and two-dimensional stable/unstable manifolds attached to them. The results are illustrated
 1365 in Figure 11. These parameterized local manifolds, when combined with the quasi-periodic
 1366 structures found through phase space sampling, provide substantial insight into the phase
 1367 space structure of the system.

1368 The interested reader can repeat these computations by running the program

1369 `lomeliPerMScript2D.m`.

1370 We remark that the computations for the two-dimensional manifolds have not been optimized
 1371 for speed, but the computations run in less than a minute.



1351 **Figure 11.** *Hyperbolic invariant objects for the Lomelí map: Top left: 2d local stable/unstable manifolds of*
 1352 *the fixed points. Quasi-periodic invariant tori (periods one and four) seen inside. Top right: 1d stable/unstable*
 1353 *manifolds attached to the fixed points (green and yellow spheres). Also shown are 1d and 2d stable/unstable*
 1354 *manifolds attached to the period four points. Bottom: the stable/unstable manifolds of fixed points and period*
 1355 *four orbit along with the period four invariant tori.*

1372 **5. Conclusions.** This work presents a framework for efficient and automatic high-order
 1373 computation of polynomial approximations of local stable/unstable manifolds attached to
 1374 periodic orbits of maps. We gave example computations illustrating the application of our
 1375 method to long periodic orbits (up to period 100 or more) to maps with nonpolynomial
 1376 nonlinearities, and to manifolds of dimensions one and two (though in principle our techniques
 1377 apply to manifolds of any dimension). Several features of the method are that it recovers the
 1378 dynamics on the manifold, that it can follow folds in the embedding, and that it admits a
 1379 natural notion of a posteriori error.

1380 We also compared the multiple-shooting parameterization method with a naive appli-
 1381 cation of the parameterization method for fixed points of the composition map. Here we
 1382 see clearly that while both methods accurately compute the local manifolds, the multiple-
 1383 shooting approach is much more efficient in terms of runtime, floating point operations, and
 1384 accuracy. Moreover, from the point of view of implementation, a major advantage of the
 1385 multiple-shooting approach is that, regardless of the period of the orbit, we deal only with
 1386 the nonlinearity of the original map. If, on the other hand, we compute compositions, we face
 1387 exponential growth of the complexity of the nonlinearity.

In practice the high-order parameterizations developed here are often “global enough” to uncover homoclinic connections. This suggests that the method could be helpful in computer-assisted existence proofs, a topic which will be the object of future study. Indeed, it seems possible to combine the techniques of [32] with the recent work of [20, 43] and the parameterization method of the present study to obtain computer-assisted proofs of homoclinic and heteroclinic connecting dynamics for infinite-dimensional systems. Another interesting project would be to apply the methods of the present work to the difficult stable/unstable manifold computations of the period five point discussed in [7]. Unfortunately, the explicit form of the map used for that study is not given in the reference (however, the authors remark that the map is an 11th-order polynomial, a fact which suggests that the multiple-shooting approach of the present work could be a great help).

Another interesting direction of future research would be to apply rigorous globalization methods such as those of [66, 78] to grow the local manifolds studied here. This could lead to a better understanding of the connecting orbit structure and topological entropy for discrete time systems.

Acknowledgments. The authors would like to thank the three anonymous referees who read the submitted version of the manuscript for making a number of helpful suggestions. The final version is much improved thanks to their efforts.

REFERENCES

- [1] P. AGUIRRE, E. J. DOEDEL, B. KRAUSKOPF, AND H. M. OSINGA, *Investigating the consequences of global bifurcations for two-dimensional invariant manifolds of vector fields*, Discrete Contin. Dyn. Syst. Ser. A, 29 (2011), pp. 1309–1344, <https://doi.org/10.3934/dcds.2011.29.1309>.
- [2] P. AGUIRRE, B. KRAUSKOPF, AND H. M. OSINGA, *Global invariant manifolds near a Shilnikov homoclinic bifurcation*, J. Comput. Dyn., 1 (2014), pp. 1–38, <https://doi.org/10.3934/jcd.2014.1.1>.
- [3] S. ANASTASSIU, T. BOUNTIS, AND A. BÄCKER, *Homoclinic Points of 2-d and 4-d Maps via the Parameterization Method*, preprint, [arXiv:1605.05521](https://arxiv.org/abs/1605.05521), 2016.
- [4] E. BELBRUNO, M. GIDEA, AND F. TOPPUTO, *Weak stability boundary and invariant manifolds*, SIAM J. Appl. Dyn. Syst., 9 (2010), pp. 1061–1089, <https://doi.org/10.1137/090780638>.
- [5] E. BELBRUNO, M. GIDEA, AND F. TOPPUTO, *Geometry of weak stability boundaries*, Qual. Theory Dyn. Syst., 12 (2013), pp. 53–66, <https://doi.org/10.1007/s12346-012-0069-x>.
- [6] M. BERZ, S. NEWHOUSE, AND A. WITTIG, *Computer assisted proof of the existence of high order periodic points*, Fields Institute Communications, (to appear).
- [7] M. BERZ AND A. WITTIG, *High period fixed points, stable and unstable manifolds, and chaos in accelerator transfer maps*, Vestnik S.-Petersburg Univ., 10 (2014), pp. 93–110.
- [8] W.-J. BEYN, *The numerical computation of connecting orbits in dynamical systems*, IMA J. Numer. Anal., 10 (1990), pp. 379–405, <https://doi.org/10.1093/imanum/10.3.379>.
- [9] W.-J. BEYN AND W. KLESS, *Numerical Taylor expansions of invariant manifolds in large dynamical systems*, Numer. Math., 80 (1998), pp. 1–38, <https://doi.org/10.1007/s002110050357>.
- [10] M. BREDEN, J. LESSARD, AND J. MIRELES JAMES, *Computation of maximal local (un)stable manifold patches by the parameterization method*, Indag. Math., 27 (2016), pp. 340–367.
- [11] M. BÜCKER, G. CORLISS, U. NAUMANN, P. HOVLAND, AND B. NORRIS, EDs., *Automatic Differentiation: Applications, Theory, and Implementations*, Lecture Notes in Comput. Sci. Eng. 50, Springer-Verlag, Berlin, 2006, <https://doi.org/10.1007/3-540-28438-9>.
- [12] X. CABRÉ, E. FONTICH, AND R. DE LA LLAVE, *The parameterization method for invariant manifolds. I. Manifolds associated to non-resonant subspaces*, Indiana Univ. Math. J., 52 (2003), pp. 283–328.
- [13] X. CABRÉ, E. FONTICH, AND R. DE LA LLAVE, *The parameterization method for invariant manifolds. II. Regularity with respect to parameters*, Indiana Univ. Math. J., 52 (2003), pp. 329–360.

- 1435 [14] X. CABRÉ, E. FONTICH, AND R. DE LA LLAVE, *The parameterization method for invariant manifolds.*
1436 III. *Overview and applications*, J. Differential Equations, 218 (2005), pp. 444–515.
- 1437 [15] M. J. CAPIŃSKI AND J. D. MIRELES JAMES, *Validated computation of heteroclinic sets*, SIAM J. Appl.
1438 Dyn. Syst., 16 (2017), pp. 375–409, <https://doi.org/10.1137/16M1060674>.
- 1439 [16] B. V. CHIRIKOV, *A universal instability of many-dimensional oscillator systems*, Phys. Rep., 52 (1979),
1440 pp. 263–379, [https://doi.org/10.1016/0370-1573\(79\)90023-1](https://doi.org/10.1016/0370-1573(79)90023-1).
- 1441 [17] J. L. CREASER, B. KRAUSKOPF, AND H. M. OSINGA, *α -flips and T-points in the Lorenz system*, Non-
1442 linearity, 28 (2015), pp. R39–R65, <https://doi.org/10.1088/0951-7715/28/3/R39>.
- 1443 [18] S. DAY, R. FRONGILLO, AND R. TREVIÑO, *Algorithms for rigorous entropy bounds and symbolic dynamics*,
1444 SIAM J. Appl. Dyn. Syst., 7 (2008), pp. 1477–1506, <https://doi.org/10.1137/070688080>.
- 1445 [19] S. DAY AND W. D. KALIES, *Rigorous computation of the global dynamics of integrodifference equations*
1446 *with smooth nonlinearities*, SIAM J. Numer. Anal., 51 (2013), pp. 2957–2983, <https://doi.org/10.1137/120903129>.
- 1447 [20] R. DE LA LLAVE AND J. MIRELES JAMES, *Parameterization of invariant manifolds by reducibility*
1448 *for volume preserving and symplectic maps*, Discrete Contin. Dyn. Syst. Ser. A, 32 (2012), pp.
1449 4321–4360, <https://doi.org/10.3934/dcds.2012.32.4321>.
- 1450 [21] M. DELLNITZ AND A. HOHMANN, *A subdivision algorithm for the computation of unstable manifolds and*
1451 *global attractors*, Numer. Math., 75 (1997), pp. 293–317, <https://doi.org/10.1007/s002110050240>.
- 1452 [22] M. DELLNITZ, O. JUNGE, W. S. KOON, F. LEKIEN, M. W. LO, J. E. MARSDEN, K. PADBERG, R. PREIS,
1453 S. D. ROSS, AND B. THIÈRE, *Transport in dynamical astronomy and multibody problems*, Internat. J.
1454 Bifur. Chaos Appl. Sci. Engrg., 15 (2005), pp. 699–727, <https://doi.org/10.1142/S0218127405012545>.
- 1455 [23] A. DELSHAMS, M. GIDEA, R. DE LA LLAVE, AND T. M. SEARA, *Geometric approaches to the problem of*
1456 *instability in Hamiltonian systems. An informal presentation*, in Hamiltonian Dynamical Systems and
1457 Applications, NATO Sci. Peace Secur. Ser. B Phys. Biophys., Springer, Dordrecht, 2008, pp. 285–336,
1458 https://doi.org/10.1007/978-1-4020-6964-2_13.
- 1459 [24] A. DELSHAMS, M. GIDEA, AND P. ROLDÁN, *Transition map and shadowing lemma for normally hyperbolic*
1460 *invariant manifolds*, Discrete Contin. Dyn. Syst., 33 (2013), pp. 1089–1112.
- 1461 [25] E. J. DOEDEL, *Lecture notes on numerical analysis of bifurcation problems*, in International Course on
1462 Bifurcations and Stability in Structural Engineering, Université Pierre et Marie Curie (Paris VI),
1463 2000.
- 1464 [26] E. J. DOEDEL AND M. J. FRIEDMAN, *Numerical computation of heteroclinic orbits*, J. Comput. Appl.
1465 Math., 26 (1989), pp. 155–170, [https://doi.org/10.1016/0377-0427\(89\)90153-2](https://doi.org/10.1016/0377-0427(89)90153-2).
- 1466 [27] E. J. DOEDEL, B. KRAUSKOPF, AND H. M. OSINGA, *Global invariant manifolds in the transition to*
1467 *preturbulence in the Lorenz system*, Indag. Math. (N.S.), 22 (2011), pp. 222–240, <https://doi.org/10.1016/j.indag.2011.10.007>.
- 1468 [28] A. DOUADY AND J. H. HUBBARD, *Étude dynamique des polynômes complexes*, Pub. Math. d’Orsay 84,
1469 Université de Paris-Sud, Dép. de Mathématique, Orsay, France, 1984.
- 1470 [29] H. R. DULLIN AND J. D. MEISS, *Quadratic volume-preserving maps: Invariant circles and bifurcations*,
1471 SIAM J. Appl. Dyn. Syst., 8 (2009), pp. 76–128, <https://doi.org/10.1137/080728160>.
- 1472 [30] V. FRANCESCHINI AND L. RUSSO, *Stable and unstable manifolds of the Hénon mapping*, J. Statist. Phys.,
1473 25 (1981), pp. 757–769, <https://doi.org/10.1007/BF01022365>.
- 1474 [31] M. J. FRIEDMAN AND E. J. DOEDEL, *Numerical computation and continuation of invariant manifolds*
1475 *connecting fixed points*, SIAM J. Numer. Anal., 28 (1991), pp. 789–808, <https://doi.org/10.1137/0728042>.
- 1476 [32] Z. GALIAS AND P. ZGLICZYŃSKI, *Infinite-dimensional Krawczyk operator for finding periodic orbits of*
1477 *discrete dynamical systems*, Internat. J. Bifur. Chaos Appl. Sci. Engrg., 17 (2007), pp. 4261–4272,
1478 <https://doi.org/10.1142/S0218127407019937>.
- 1479 [33] G. GÓMEZ, W. S. KOON, M. W. LO, J. E. MARSDEN, J. MASDEMONT, AND S. D. ROSS, *Connecting*
1480 *orbits and invariant manifolds in the spatial restricted three-body problem*, Nonlinearity, 17 (2004),
1481 pp. 1571–1606, <https://doi.org/10.1088/0951-7715/17/5/002>.
- 1482 [34] J. GONZALEZ AND J. D. MIRELES JAMES, *High-Order Parameterization of Stable/Unstable Mani-*
1483 *folds for Long Periodic Orbits of Maps*, preprint, 2017, [http://cosweb1.fau.edu/~jmirelesjames/](http://cosweb1.fau.edu/~jmirelesjames/periodicParmManifoldPage.html)
1484 [periodicParmManifoldPage.html](http://cosweb1.fau.edu/~jmirelesjames/periodicParmManifoldPage.html).

- 1488 [35] R. H. GOODMAN AND J. K. WRÓBEL, *High-order bisection method for computing invariant manifolds*
1489 *of two-dimensional maps*, Internat. J. Bifur. Chaos Appl. Sci. Engrg., 21 (2011), pp. 2017–2042,
1490 <https://doi.org/10.1142/S0218127411029604>.
- 1491 [36] J. M. GREENE, R. S. MACKEY, F. VIVALDI, AND M. J. FEIGENBAUM, *Universal behaviour in families of*
1492 *area-preserving maps*, Phys. D, 3 (1981), pp. 468–486, [https://doi.org/10.1016/0167-2789\(81\)90034-8](https://doi.org/10.1016/0167-2789(81)90034-8).
- 1493 [37] J. GUCKENHEIMER AND A. VLADIMIRSKY, *A fast method for approximating invariant manifolds*, SIAM
1494 J. Appl. Dyn. Syst., 3 (2004), pp. 232–260, <https://doi.org/10.1137/030600179>.
- 1495 [38] A. HARO, *Automatic Differentiation Methods in Computational Dynamical Systems: Invariant Manifolds*
1496 *and Normal Forms of Vector Fields at Fixed Points*, manuscript.
- 1497 [39] A. HARO, M. CANADELL, J.-L. FIGUERAS, A. LUQUE, AND J. M. MONDELO, *The Parameterization*
1498 *Method for Invariant Manifolds: From Rigorous Results to Effective Computations*, Appl. Math. Sci.
1499 195, Springer, Cham, 2016, <https://doi.org/10.1007/978-3-319-29662-3>.
- 1500 [40] M. E. HENDERSON, *Computing invariant manifolds by integrating fat trajectories*, SIAM J. Appl. Dyn.
1501 Syst., 4 (2005), pp. 832–882, <https://doi.org/10.1137/040602894>.
- 1502 [41] M. HÉNON, *A two-dimensional mapping with a strange attractor*, Comm. Math. Phys., 50 (1976),
1503 pp. 69–77.
- 1504 [42] S. HITMEYER, B. KRAUSKOPF, AND H. M. OSINGA, *Interactions of the Julia set with critical and*
1505 *(un)stable sets in an angle-doubling map on $\mathbb{C}\setminus\{0\}$* , Internat. J. Bifur. Chaos Appl. Sci. Engrg., 25
1506 (2015), 1530013, <https://doi.org/10.1142/S021812741530013X>.
- 1507 [43] J. D. M. JAMES, *Fourier–Taylor approximation of unstable manifolds for compact maps: Numerical*
1508 *implementation and computer assisted error bounds*, Found. Comput. Math., 2016, pp. 1–57 <https://doi.org/10.1-007/s10208-016-9325-9>.
- 1509 [44] T. JOHNSON AND W. TUCKER, *A note on the convergence of parametrised nonresonant invariant mani-*
1510 *folds*, Qual. Theory Dyn. Syst., 10 (2011), pp. 107–121, <https://doi.org/10.1007/s12346-011-0040-2>.
- 1511 [45] À. JORBA AND M. ZOU, *A software package for the numerical integration of ODEs by means of high-order*
1512 *Taylor methods*, Experiment. Math., 14 (2005), pp. 99–117, <http://projecteuclid.org/getRecord?id=euclid.em/1120145574>.
- 1513 [46] D. E. KNUTH, *The Art of Computer Programming. Vol. 2: Seminumerical Algorithms*, 2nd ed., Addison-
1514 Wesley Ser. Comput. Sci. Inform. Process., Addison-Wesley, Reading, MA, 1981.
- 1515 [47] W. S. KOON, M. W. LO, J. E. MARSDEN, AND S. D. ROSS, *Low energy transfer to the moon*, Celestial
1516 Mech. Dyn. Astronom., 81 (2001), pp. 63–73, <https://doi.org/10.1023/A:1013359120468>.
- 1517 [48] B. KRAUSKOPF AND H. OSINGA, *Globalizing two-dimensional unstable manifolds of maps*, Internat. J.
1518 Bifur. Chaos Appl. Sci. Engrg., 8 (1998), pp. 483–503, <https://doi.org/10.1142/S0218127498000310>.
- 1519 [49] B. KRAUSKOPF AND H. OSINGA, *Growing 1D and quasi-2D unstable manifolds of maps*, J. Comput.
1520 Phys., 146 (1998), pp. 404–419, <https://doi.org/10.1006/jcph.1998.6059>.
- 1521 [50] B. KRAUSKOPF AND H. M. OSINGA, *Computing geodesic level sets on global (un)stable manifolds of vector*
1522 *fields*, SIAM J. Appl. Dyn. Syst., 2 (2003), pp. 546–569, <https://doi.org/10.1137/030600180>.
- 1523 [51] B. KRAUSKOPF AND H. M. OSINGA, *The Lorenz manifold as a collection of geodesic level sets*, Nonlin-
1524 earity, 17 (2004), pp. C1–C6, <https://doi.org/10.1088/0951-7715/17/1/000>.
- 1525 [52] B. KRAUSKOPF, H. M. OSINGA, E. J. DOEDEL, M. E. HENDERSON, J. GUCKENHEIMER,
1526 A. VLADIMIRSKY, M. DELLNITZ, AND O. JUNGE, *A survey of methods for computing (un)stable*
1527 *manifolds of vector fields*, Internat. J. Bifur. Chaos Appl. Sci. Engrg., 15 (2005), pp. 763–791,
1528 <https://doi.org/10.1142/S0218127405012533>.
- 1529 [53] H. E. LOMELÍ, J. D. MEISS, AND K. E. LENZ, *Quadratic volume preserving maps: An exten-*
1530 *sion of a result of Moser*, Regul. Chaotic Dyn., 3 (1998), pp. 122–131, <https://doi.org/10.1070/rd1998v003n03ABEH000085>.
- 1531 [54] H. E. LOMELÍ AND J. D. MEISS, *Quadratic volume-preserving maps*, Nonlinearity, 11 (1998), pp. 557–574,
1532 <https://doi.org/10.1088/0951-7715/11/3/009>.
- 1533 [55] H. E. LOMELÍ AND J. D. MEISS, *Heteroclinic intersections between invariant circles of volume-preserving*
1534 *maps*, Nonlinearity, 16 (2003), pp. 1573–1595, <https://doi.org/10.1088/0951-7715/16/5/302>.
- 1535 [56] H. E. LOMELÍ AND J. D. MEISS, *Resonance zones and lobe volumes for exact volume-preserving maps*,
1536 Nonlinearity, 22 (2009), pp. 1761–1789, <https://doi.org/10.1088/0951-7715/22/8/001>.
- 1537 [57] H. E. LOMELÍ, J. D. MEISS, AND R. RAMÍREZ-ROS, *Canonical Melnikov theory for diffeomorphisms*,
1538 Nonlinearity, 21 (2008), pp. 485–508, <https://doi.org/10.1088/0951-7715/21/3/007>.

- 1542 [58] R. S. MACKAY, *A renormalisation approach to invariant circles in area-preserving maps*, Phys. D, 7
1543 (1983), pp. 283–300, [https://doi.org/10.1016/0167-2789\(83\)90131-8](https://doi.org/10.1016/0167-2789(83)90131-8).
- 1544 [59] K. MAKINO AND M. BERZ, *Taylor models and other validated functional inclusion methods*, Int. J. Pure
1545 Appl. Math., 4 (2003), pp. 379–456.
- 1546 [60] J. J. MASDEMONT, *High-order expansions of invariant manifolds of libration point orbits with applications
1547 to mission design*, Dyn. Syst., 20 (2005), pp. 59–113, <https://doi.org/10.1080/14689360412331304291>.
- 1548 [61] J. MIRELES JAMES, *Polynomial approximation of one parameter families of (un)stable manifolds with
1549 rigorous computer assisted error bounds*, Indag. Math., 26 (2015), pp. 225–265.
- 1550 [62] J. D. MIRELES JAMES, *Quadratic volume-preserving maps: (Un)stable manifolds, hyperbolic dynamics,
1551 and vortex-bubble bifurcations*, J. Nonlinear Sci., 23 (2013), pp. 585–615.
- 1552 [63] J. D. MIRELES JAMES, *Computer assisted error bounds for linear approximation of (un)stable manifolds
1553 and rigorous validation of higher dimensional transverse connecting orbits*, Comm. Nonlinear Sci.
1554 Numer. Simul., 22 (2015), pp. 1102–1133.
- 1555 [64] J. D. MIRELES JAMES AND H. LOMELÍ, *Computation of heteroclinic arcs with application to the volume
1556 preserving Hénon family*, SIAM J. Appl. Dyn. Syst., 9 (2010), pp. 919–953, [https://doi.org/10.1137/
1557 090776329](https://doi.org/10.1137/090776329).
- 1558 [65] J. D. MIRELES JAMES AND K. MISCHAIKOW, *Rigorous a posteriori computation of (un)stable manifolds
1559 and connecting orbits for analytic maps*, SIAM J. Appl. Dyn. Syst., 12 (2013), pp. 957–1006, [https://doi.org/10.1137/
1560 12088224X](https://doi.org/10.1137/12088224X).
- 1561 [66] S. NEWHOUSE, M. BERZ, J. GROTE, AND K. MAKINO, *On the estimation of topological entropy on sur-
1562 faces*, in Geometric and Probabilistic Structures in Dynamics, Contemp. Math. 469, AMS Providence,
1563 RI, 2008, pp. 243–270, <https://doi.org/10.1090/conm/469/09170>.
- 1564 [67] C. ROBINSON, *Dynamical systems: Stability, Symbolic Dynamics, and Chaos*, Stud. Adv. Math., CRC
1565 Press, Boca Raton, FL, 1998.
- 1566 [68] M. ROMERO-GÓMEZ, E. ATHANASSOULA, J. J. MASDEMONT, AND C. GARCÍA-GÓMEZ, *Invariant man-
1567 ifolds as building blocks for the formation of spiral arms and rings in barred galaxies*, in Chaos in
1568 Astronomy, Astrophys. Space Sci. Proc., Springer, Berlin, 2009, pp. 85–92.
- 1569 [69] M. ROMERO-GÓMEZ, P. SÁNCHEZ-MARTÍN, AND J. J. MASDEMONT, *How invariant manifolds form
1570 spirals and rings in barred galaxies*, Butl. Soc. Catalana Mat., 29 (2014), pp. 51–75.
- 1571 [70] C. SIMO, *On the analytical and numerical approximation of invariant manifolds*, in Modern Methods in
1572 Celestial Mechanics, Ecole de Printemps d’Astrophysique de Goutelas (France), D. Benest, and C.
1573 Froeschle, eds., Gif-sur-Yvette: Editions Frontières, 1990, pp. 285–329.
- 1574 [71] S. SMALE, *Differentiable dynamical systems*, Bull. Amer. Math. Soc., 73 (1967), pp. 747–817.
- 1575 [72] M. TANTARDINI, E. FANTINO, Y. REN, P. PERGOLA, G. GÓMEZ, AND J. J. MASDEMONT, *Spacecraft
1576 trajectories to the L_3 point of the Sun–Earth three-body problem*, Celestial Mech. Dynam. Astronom.,
1577 108 (2010), pp. 215–232, <https://doi.org/10.1007/s10569-010-9299-x>.
- 1578 [73] W. TUCKER, *A rigorous ODE solver and Smale’s 14th problem*, Found. Comput. Math., 2 (2002),
1579 pp. 53–117, <http://dx.doi.org/10.1007/s002080010018>.
- 1580 [74] W. TUCKER, *Validated Numerics: A Short Introduction to Rigorous Computations*, Princeton University
1581 Press, Princeton, NJ, 2011.
- 1582 [75] W. TUCKER AND D. WILCZAK, *A rigorous lower bound for the stability regions of the quadratic map*,
1583 Phys. D, 238 (2009), pp. 1923–1936, <https://doi.org/10.1016/j.physd.2009.06.020>.
- 1584 [76] J. B. VAN DEN BERG, J. D. MIRELES JAMES, AND C. REINHARDT, *Computing (un)stable manifolds
1585 with validated error bounds: Non-resonant and resonant spectra*, J. Nonlinear Sci., 26 (2016), pp.
1586 1055–1095, <https://doi.org/10.1007/s00332-016-9298-5>.
- 1587 [77] D. WILCZAK, *Uniformly hyperbolic attractor of the Smale–Williams type for a Poincaré map in the
1588 Kuznetsov system*, SIAM J. Appl. Dyn. Syst., 9 (2010), pp. 1263–1283, [https://doi.org/10.1137/
1589 100795176](https://doi.org/10.1137/100795176).
- 1590 [78] A. WITTIG, M. BERZ, J. GROTE, K. MAKINO, AND S. NEWHOUSE, *Rigorous and accurate enclosure
1591 of invariant manifolds on surfaces*, Regul. Chaotic Dyn., 15 (2010), pp. 107–126, [https://doi.org/10.
1592 1134/S1560354710020024](https://doi.org/10.1134/S1560354710020024).
- 1593 [79] J. K. WRÓBEL AND R. H. GOODMAN, *High-order adaptive method for computing two-dimensional in-
1594 variant manifolds of three-dimensional maps*, Commun. Nonlinear Sci. Numer. Simul., 18 (2013),
1595 pp. 1734–1745, <https://doi.org/10.1016/j.cnsns.2012.10.017>.